Satellite Observations of the Wind Jets off the Pacific Coast of Central America. Part II: Regional Relationships and Dynamical Considerations

DUDLEY B. CHELTON, MICHAEL H. FREILICH, AND STEVEN K. ESBENSEN

College of Oceanic and Atmospheric Sciences, Oregon State University, Corvallis, Oregon

(Manuscript received 15 September 1998, in final form 12 July 1999)

ABSTRACT

Satellite estimates of winds at 10 m above the sea surface by the NASA scatterometer (NSCAT) during the 9-month period October 1996–June 1997 are analyzed to investigate the correlations between the three major wind jets along the Pacific coast of Central America and their relationships to the wind and pressure fields in the Inter-American Seas and eastern tropical Pacific. Comparisons with sea level pressure confirm the conventional view that Tehuantepec wind variations are driven by pressure variations in the Gulf of Mexico associated with North American cold-air outbreaks. The three jets sometimes developed sequentially from north to south. Statistically, however, the Papagayo and Panama jets were poorly correlated with variations of the Tehuantepec jet over the NSCAT observational period. The Papagayo and Panama jets were significantly correlated with each other and were coupled to coherent variations of the trade winds extending from the Caribbean Sea to the eastern tropical Pacific.

The detailed structures of the wind fields within the three jets are examined to infer dynamical balances within the jets. After leaving the coast, the northerly Tehuantepec and Panama jets turn anticyclonically toward the west in manners that are consistent with jets that are inertially balanced at the coast and become progressively more geostrophically balanced with increasing distance from the coast. There is no evidence of anticyclonic turning of the easterly Papagayo jet, suggesting that the winds may remain in approximate geostrophic balance through the gap over the Nicaraguan lake district.

NSCAT observations are compared with operational analyses by ECMWF to investigate the detailed structures of the wind fields over the Gulfs of Tehuantepec, Papagayo, and Panama. Systematic differences between the NSCAT observations and the ECMWF analyses of the divergent off-axis fanning of all three jets suggest that there may be systematic errors in parameterizations of boundary layer processes in the ECMWF ''first-guess'' fields in these data-sparse regions.

1. Introduction

The existence of three major intermittent wind jets over the Gulfs of Tehuantepec, Papagayo, and Panama along the west coast of Central America[1] was documented in the literature by the end of the third decade of this century (Frankenfield 1917; Chapel 1927; Hurd 1929). It is well established that the Tehuantepec jet is triggered by relatively high pressure in the Gulf of Mexico that is associated with cold-air outbreaks from the Great Plains of North America (Hurd 1929; Parmenter 1970; Schultz et al. 1997; Steenburgh et al. 1998). Not all cold fronts penetrate far enough south to affect the Papagayo and Panama jets (Schultz et al. 1998). Those that do, however, sequentially trigger the Papagayo and Panama jets as the high pressure moves into the southwestern Caribbean Sea. Schultz et al. (1997) have described the evolution of such an event that occurred in March 1993 when the Papagayo and Panama jets were initiated 12 h after the onset of the Tehuantepec jet. This north-to-south triggering, first suggested by Hurd (1929), has become widely accepted as the primary mechanism for generation of the Papagayo and Panama jets during winter.

Until recently, wind observations have not been available with sufficient spatial and temporal coverage to investigate the generality of the conventional view that variations of the Papagayo and Panama jets are linked to the Tehuantepec jet. In a companion paper to this study, Chelton et al. (2000, referred to hereafter as CFE) analyzed satellite observations of surface winds by the National Aeronautics and Space Administration (NASA) scatterometer (NSCAT) over the 9-month period October 1996–June 1997 to describe the evolution of the three jets during three representative case studies.

[1] For a map of the topography and geographical locations referred to in this paper, see Fig. 1 of the companion paper by Chelton et al. (2000).

Corresponding author address: Dudley B. Chelton, College of Oceanic and Atmospheric Sciences, Oregon State University, 104 Ocean Admin Building, Corvallis, OR 97331-5503.
E-mail: chelton@oce.orst.edu

A Tehuantepec jet developed in all three case studies immediately after increased sea level pressure (SLP) over the Gulf of Mexico associated with a cold surge of midlatitude origin. In a December 1996 case study and during the early stages of a November 1996 case study, the Papagayo and Panama jets were sequentially triggered after the Tehuantepec jet in accord with the conventional view. However, in the late stages of the November case study and throughout a March 1997 case study, the Papagayo and Panama jets were strongly influenced by tropical atmospheric systems (a tropical cyclone in November and intensified trade winds in March) that had little apparent relationship with the Tehuantepec jet. High pressure systems of midlatitude origin are evidently not the only mechanism for generation of the Papagayo and Panama jets. The objective of this study is to quantify the similarities and differences in the generation, development, and regional interactions of the three jets based on statistical analyses of the NSCAT winds and reanalyzed SLP fields produced by the National Centers for Environmental Prediction (NCEP).

The NSCAT observational period can be placed in the context of climatological conditions from the synthesis of historical analyses by Schultz et al. (1998). They concluded that cold air from the Great Plains of North America typically surges southward into the Gulf of Mexico about a dozen times per year between October and March. The maximum frequency and intensity generally occur in January and February. These cold surges last anywhere from 1 day to 2 weeks. During the 9-month NSCAT data record, at least a dozen strong jets and an even larger number of moderately strong jets were observed over the Gulf of Tehuantepec (see Figs. 10 and 13 of CFE). In terms of the number of Tehuantepec wind events, the NSCAT observational period thus appears to be representative of climatological conditions. As climatological statistics are not available for the Papagayo and Panama jets, it is more difficult to assess whether the 1996–97 jet season was typical of climatological conditions at these two lower-latitude locations. We note, however, that the Papagayo and Panama jets were both very active during the NSCAT observational period (see Figs. 10 and 13 of CFE). The NSCAT dataset therefore seems adequate to investigate the relationships between the three jets.

The paper proceeds as follows. The strengths and limitations of the NSCAT dataset are briefly summarized in section 2. Regional relationships between each of the jets and the surrounding wind field are examined from correlation analyses in section 3. The generation mechanisms for the jets are investigated in section 4 from correlations of the wind jets with SLP fields over the Inter-American Seas[2] and the eastern tropical Pacific. The spatial structures of the three jets are examined in section 5 to draw inferences about the dynamics of the jets. Particular emphasis is devoted to investigating the divergent off-axis fanning of the jets near the coast and the anticyclonic turning of the cores of the jets after leaving the coast.

2. Scatterometry

As the scatterometer is a relatively new observational tool for the study of near-surface winds, the measurement technique is briefly summarized here. A detailed description is given in CFE. The scatterometer is a microwave radar that infers near-surface winds in near all-weather conditions from measurements of the roughness of the sea surface at centimetric wavelengths. The orientations of these wavelets relative to the wind direction and the amplitude dependence of the wavelets on wind speed allow a determination of both wind speed and direction with a spatial resolution of about 25 km. The NSCAT wind retrieval algorithm is calibrated to a reference height of 10 m above the sea surface.

The accuracies of NSCAT estimates of 10-m winds have been shown to be about the same as those of high-quality buoy measurements (see, e.g., Freilich and Dunbar 1999; the appendix of CFE; Freilich and Vanhoff 2000, manuscript submitted to *J. Atmos. Oceanic Technol.*). The unique contribution of scatterometry is the global coverage that far surpasses that of any other observational system for measuring near-surface winds. Over the Inter-American Seas and eastern tropical Pacific regions of interest in this study, NSCAT measured approximately 10 000 wind observations per day (see Fig. 2 of CFE) with a spatial resolution of about 25 km. The NSCAT data thus provide unprecedented spatial and temporal coverage of the three Central American wind jets and the surrounding wind field.

As with all observational systems, however, the NSCAT data are not without limitations. The primary limitation of NSCAT data is the sampling errors that arise from the NSCAT limited measurement swath (see Fig. 3 of CFE). The average revisit interval over the domain of interest in this study was 23.5 h. The NSCAT data therefore obviously cannot resolve the detailed development of rapidly evolving wind events. Moreover, the NSCAT observations must be temporally smoothed to construct maps of the 10-m wind field with relatively complete spatial coverage.

To maximize the temporal resolution in time series constructed from NSCAT data, the correlation statistics in sections 3 and 4 of this study are computed from daily averaged winds over $1^\circ \times 1^\circ$ areas. To reduce the gaps in spatial coverage, the structures of the wind jets in section 5 are investigated from 2-day composite averages of NSCAT winds over $1^\circ \times 1^\circ$ areas.

[2] By definition, the Inter-American Seas comprise the Gulf of Mexico, the Caribbean Sea, and the Straits of Florida.

3. Correlation scales of the wind jets

The statistical description of the individual jets by CFE clearly showed that each jet was distinctive in character during the 9-month NSCAT observational period. The Tehuantepec jet was more energetic and transient than the other two jets. Consistent with the statistical analysis of 18 yr of coastal wind observations by Chapel (1927) during the period 1908–26, the Panama winds were the least energetic and the most heavily influenced by southwesterly onshore flow during October and November 1996 in association with the late stages of the 1996 Central American monsoon season. The winds in the Papagayo jet were the most persistent and the most consistently offshore. The correlations of each of the jets with each other and with the surrounding wind field are examined in this section.

A simple scalar measure of the correlation between two vector time series has been developed by Jupp and Mardia (1980; see also Crosby et al. 1993; Breaker et al. 1994; Freilich and Dunbar 1999). The vector squared correlation between a pair of two-dimensional vector time series is computed from the orthogonal components of the vectors as described by Crosby et al. (1993). The magnitude of the vector squared correlation ranges from a value of zero when the two vector time series are independent to a value of 2.0 when the two orthogonal components are each linearly related. A perfect vector squared correlation of 2.0 occurs when the two vector time series differ only by a constant multiplicative factor in speed and a constant offset in direction.

The statistical significance of the sample estimate of any statistic is determined from the probability distribution of the sample statistic. For the standard squared correlation between two scalar time series, N^* times the sample estimate of the squared correlation is approximately χ^2 distributed with 1 degree of freedom, where N^* is the number of independent observations from which the sample squared correlation is computed. Crosby et al. (1993) show that N^* times the sample estimate of the vector squared correlation is approximately χ^2 distributed with 4 degrees of freedom.

The serial correlation of the major-axis wind component evident from the autocorrelations in Fig. 14 of CFE indicates that the N sample observations are not all statistically independent, that is, that $N^* < N$. Methods for estimating N^* have been developed for the standard scalar correlation (e.g., Chelton 1983). However, a formalism for estimating N^* has not yet been developed for vector squared correlations. In lieu of such a formalism, the values of N^* reported below for sample estimates of the standard squared correlations were also used for sample estimates of the vector squared correlations. While not completely satisfactory, this is certainly better than the overly optimistic assumption that $N^* = N$. The values of N^* were estimated by the long-lag correlation method summarized in Chelton (1983) and the significance levels of the scalar squared correlations and vector squared correlations were estimated from the χ^2 distribution based on these values of N^*.

TABLE 1. The vector squared correlations between the vector wind time series (upper-right triangle) and the standard squared correlations between the scalar major-axis wind component time series (lower-left triangle) at the three wind jet locations. The vector time series and major-axis wind component time series are shown in Figs. 10 and 13 of CFE. The numbers in parentheses are estimates of the 99% significance levels of the squared correlations computed based on the effective degrees of freedom N^* in the sample data records estimated as described in the text.

	Tehuantepec	Papagayo	Panama
Tehuantepec	—	0.06 (0.22)	0.02 (0.17)
Papagayo	0.04 (0.11)	—	0.37 (0.31)
Panama	0.01 (0.09)	0.42 (0.16)	—

a. Wind correlations

The zero-lag vector squared correlations between the vector winds in the three jets over the full 9-month data record October 1996–June 1997 are listed in the upper-right triangle of Table 1; the zero-lag scalar squared correlations between the major-axis wind components (see Fig. 13 of CFE) at the three locations are listed in the lower-left triangle. Each of these squared correlations is based on $N = 136$ co-occurring daily averaged observations during the 9-month period. The values of N^* estimated for the major-axis wind component cross correlations are 61 for Tehuantepec–Papagayo, 78 for Tehuantepec–Panama, and 43 for Papagayo–Panama. The lower value of N^* for the Papagayo–Panama cross correlation reflects the energetic and highly correlated low-frequency seasonal variability at both locations (see Fig. 13 of CFE). The numbers in parentheses in Table 1 represent the estimated 99% significance levels for the various squared correlations based on these values of N^*. Sample squared correlations must exceed these critical values to be statistically significant with 99% confidence.

The table quantifies the visual impressions from the vector wind time series and scalar major-axis wind component time series shown in Figs. 10 and 13 of CFE. The Papagayo and Panama jets are significantly correlated with each other but neither is significantly correlated with the Tehuantepec jet. An analysis of correlations out to lags of ± 3 weeks (not listed in the table) concludes that the Papagayo and Panama jets are not significantly correlated with the Tehuantepec jet at any lags. Cold-air outbreaks linked to the Tehuantepec jet evidently account for very little of the variability of the Papagayo and Panama jets.

A more complete description of the space–time correlation structure of Tehuantepec winds is given in Fig. 1, which shows the R^2 values obtained from time-lagged multivariate regression of the major-axis component of Tehuantepec winds over the 9-month data record onto a constant offset and the two orthogonal wind compo-

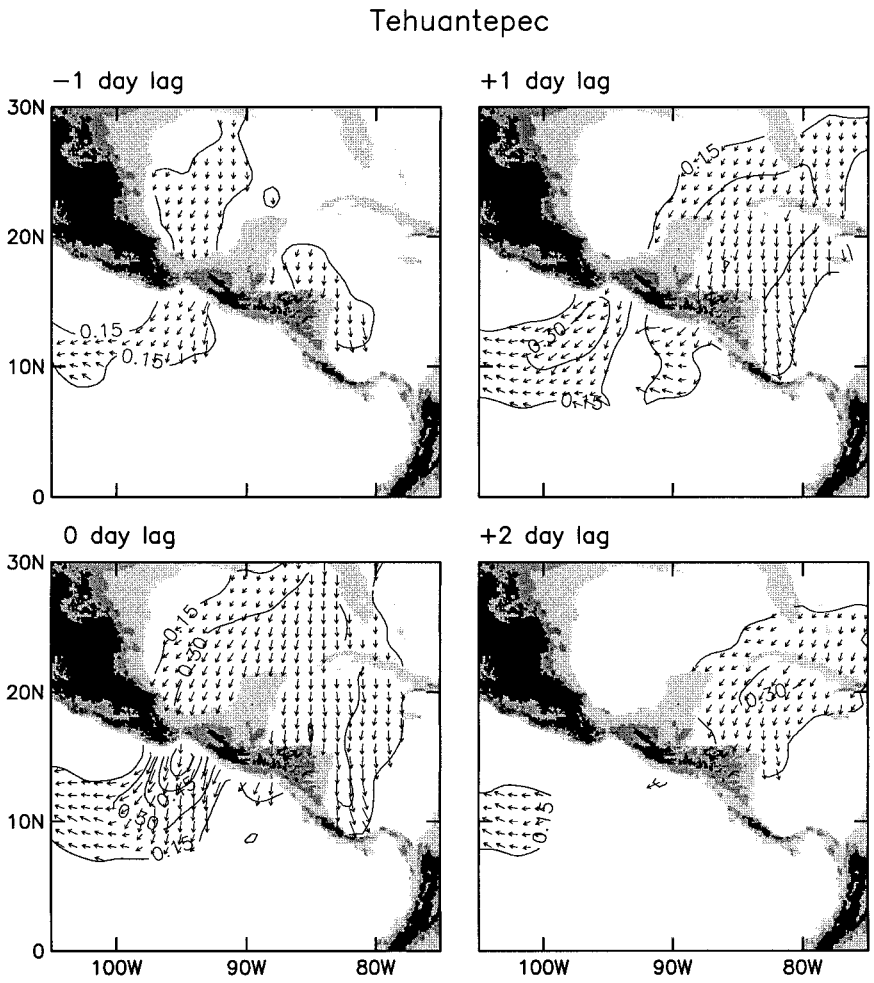

FIG. 1. Maps of the multivariate regression of the major-axis component of winds in the Tehuantepec jet at 15°N, 95°W onto orthogonal components of the vector velocity on a 1° × 1° grid at lags of −1, 0, +1, and +2 days. Negative (positive) lags correspond to Tehuantepec winds lagging (leading) the winds on the 1° grid. The contours correspond to the skills (R^2 values) of the regressions and the vectors were constructed from the pair of regression coefficients for the wind components at each 1° grid point. For clarity of presentation, regression vectors are shown only at grid locations for which the R^2 value exceeds 0.15, which corresponds to the typical 99% significance level of the sample R^2 values. The three increasingly dark shades of gray over land correspond, respectively, to topographic elevations below 300 m, between 300 and 1200 m, and above 1200 m.

nents at each 1° grid point over the Inter-American Seas and eastern tropical Pacific for lags of −1, 0, +1, and +2 days. The sign convention adopted here is that negative (positive) lags correspond to Tehuantepec winds lagging (leading) the winds on the 1° grid. The R^2 value is equivalent to the square of the correlation between the regression estimate and the observed wind in the Tehuantepec jet. The vectors on each plot indicate the direction of the winds at the corresponding grid point that are correlated with variations in the Tehuantepec wind jet. The product of N^* times the sample R^2 values for the two-parameter multivariate regressions is approximately χ^2 distributed with 2 degrees of freedom. For the 99% significance levels considered here, the corresponding critical values for the R^2 estimates are typically about 0.15. For this reason, as well as to aid the eye in identifying the important patterns of correlation, the R^2 values in Fig. 1 are contoured only in regions where $R^2 > 0.15$.

The regression maps confirm the weak correlation of the Tehuantepec jet with the Papagayo and Panama jets. At all lags shown in Fig. 1, the R^2 values are not statistically significant at the 99% confidence level in the regions of the Papagayo and Panama gap outflow. The magnitudes of the R^2 values do not increase at lags longer than are shown here. This again emphasizes the fact that the conventional view that high-SLP systems over the Inter-American Seas generate Papagayo and

Panama wind events a day or so after triggering a Tehuantepec wind event does not account for significant fractions of the variances of the winds in the vicinities of the Papagayo and Panama jets. On the Pacific side of Central America, the region of high correlation with Tehuantepec winds is restricted to the downwind extension of the Tehuantepec jet, which turns anticyclonically westward within a few hundred kilometers of the coast.

An interesting feature in the regression map for lag +1 day is the patch of small but statistically significant ($R^2 \approx 0.2$) winds centered to the east of the Tehuantepec jet and west of the Papagayo jet near 10°N, 90°W. This feature appears to be unrelated to the Papagayo jet since the region of significant correlation does not extend eastward to the gap outflow from the Nicaraguan lake district. The winds in this offshore region may represent a response to variations of SLP in the eastern tropical Pacific from airmass adjustments associated with the flow through the Tehuantepec gap.

The abrupt increase in the magnitudes of the R^2 values over most of the Gulf of Mexico between lag −1 day and lag zero emphasizes the abrupt appearance of the cold fronts that trigger Tehuantepec winds. This is further evident from the smaller R^2 values at lag −1 day than at +1 day in the downstream extension of the Tehuantepec jet. This asymmetry in the lagged R^2 values downstream of the gap indicates that, after a rapid onset, the Tehuantepec jet typically persists for about a day.

The sequence of lagged regression maps in Fig. 1 shows the expected association of the Tehuantepec wind events with synoptic weather patterns that migrate from west to east across the Gulf of Mexico and northwest Caribbean Sea. At lag −1 day, R^2 values of ~0.2 extend north of the Tehuantepec gap across the Gulf of Mexico and southwestward of the gap into the Pacific. At zero lag, the R^2 values increase to 0.3–0.4 over a broad region of the southeastern Gulf of Mexico and western Caribbean Sea. At lags of +1 and +2 days, the high pressure systems and associated northerly winds continue to move eastward across the Gulf of Mexico and the Caribbean Sea.

The region of significant R^2 values in the Caribbean Sea is restricted to the far western Caribbean where the weather systems that trigger Tehuantepec wind events generate northerly or north-northwesterly winds at lags of 0 and +1 days. While this wind direction does not preclude the possibility of generating flow through the Papagayo gap, northerly winds are not optimally aligned for the southeast-to-northwest orientation of the Nicaraguan lake district (see the shaded topography in Fig. 1; see also Fig. 1 of CFE for a more detailed map of the Central American topography). The insignificant R^2 values over the southern Caribbean Sea in the regression maps in Fig. 1 indicate that the northerly winds seldom penetrate sufficiently far south to create the cross-isthmus flow necessary for the generation of a Panama wind jet.

The space–time correlation patterns associated with the Papagayo and Panama wind jets are very different from those associated with the Tehuantepec wind jet. The scalar squared correlation and the vector squared correlation between Papagayo and Panama winds are both about 0.4, which is statistically significant for both correlations (see Table 1). Maps of the R^2 values obtained from regression of the major-axis wind component in each jet over the 9-month data record onto the two components of vector winds at each 1° grid point over the region of interest are shown in Figs. 2 and 3 for lags of −1, 0, and +1 days. As in Fig. 1, contours are shown only in regions where $R^2 > 0.15$.

Unlike the regression maps for Tehuantepec in Fig. 1, the regression maps for Papagayo and Panama at lags of −1 and +1 day are essentially the same as the zero-lag maps, except that the magnitudes of the R^2 values are somewhat smaller, especially in the immediate vicinities of the wind jets. The symmetries of the R^2 values and the regression vectors for lags of −1 and +1 days are consistent with the much greater persistence of the Papagayo and Panama wind jets noted by CFE from the longer timescales of the autocorrelation functions (see Fig. 14 of CFE). The Papagayo and Panama regression maps for lags longer than those shown in Figs. 2 and 3 confirm the poor correlation of these wind jets with the winds over the Gulf of Tehuantepec at all lags.

The insignificant R^2 values throughout the Gulf of Mexico in Figs. 2 and 3 imply that the Papagayo and Panama wind jets are decoupled from low-level atmospheric variability at midlatitudes. This is also true at lags longer than those shown in Figs. 2 and 3, further confirming the weak association of the variability of these two wind jets with cold-air outbreaks over the Gulf of Mexico.

The broad zonal bands of high R^2 values in Figs. 2 and 3 suggest that the Papagayo and Panama jets are both associated with variations in the trade winds that span from the Caribbean to the Pacific. This speculation about cross-isthmus covariability of the trade winds is confirmed from correlation analysis. The correlation between Pacific trade winds at 100°W, 9°N and Caribbean trade winds at 80°W, 12°N is maximum (0.64) when variations in Caribbean trade winds lead Pacific trade winds by 2 days. The apparent propagation of trade wind variations from the Caribbean to the Pacific is a very intriguing result that merits a detailed analysis that is beyond the scope of this study.

The orientations of the regression vectors in the western Caribbean Sea offer a possible suggestion for why the Papagayo and Panama wind jets are not more highly correlated with each other. The Panama jet is associated with northerly winds over the southern Caribbean Sea while the Papagayo jet is associated with winds that have a more easterly component over the central and southern Caribbean Sea. The more easterly orientation of the Caribbean winds associated with the Papagayo jet is more optimally aligned for the southeast-to-north-

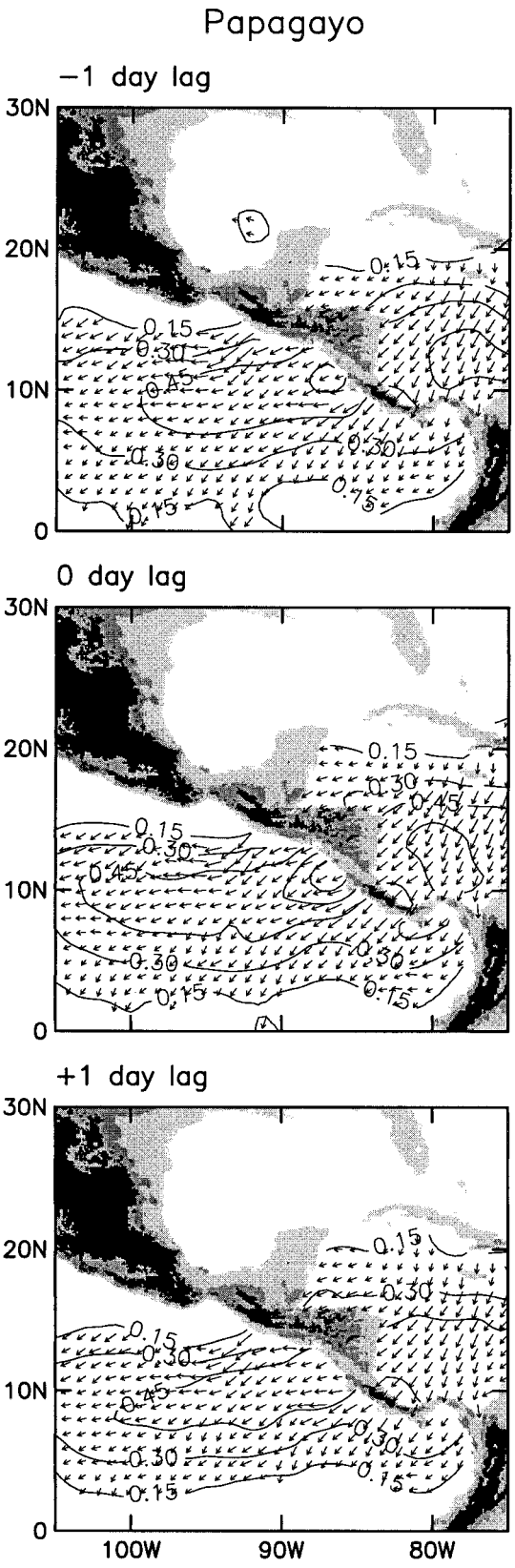

FIG. 2. The same as Fig. 1 except for regressions of the major-axis component of the Papagayo jet at 11°N, 87°W onto vector winds on a 1° × 1° grid at lags of −1, 0, and +1 days.

west orientation of the gap in the Nicaraguan lake district noted above; the ~750-m high mountains northeast of this gap would tend to block northerly flow from the Caribbean.

A subtle difference between the Pacific region of the Papagayo and Panama regression maps in Figs. 2 and 3 reveals another noteworthy distinction between the two wind jets. The Papagayo winds are associated with intensifications of easterly winds downstream from the Gulf of Papagayo centered along the mean axis of the northeast trade winds at about 10°N in this far-eastern region of the Pacific (see Fig. 11a of CFE). In comparison, the highest R^2 values for the Panama jet occur at a somewhat lower latitude centered along the mean axis of the intertropical convergence zone at about 8°N. The Panama winds thus tend to be associated with an equatorward translation of the axis of the northeast trade winds in the eastern tropical Pacific.

b. Nonseasonal wind correlations

It was noted by CFE that approximately one-third and one-half of the variances of the Papagayo and Panama jets, respectively, consisted of low-frequency seasonal variations. A question that naturally arises is the degree to which the correlation structures in the regression maps in Figs. 1–3 are dominated by these energetic seasonal variations. Of particular interest is the question of whether the energetic seasonal variability of the Papagayo and Panama jets might be obscuring correlations of these two lower-latitude jets with the Tehuantepec jet on the shorter timescales that are characteristic of episodic cold-air outbreaks.

To address these questions, the seasonal variability of vector velocities in each 9-month time series of 1°-gridded NSCAT winds was estimated by separately regressing each wind component onto the sum of annual and semiannual harmonics. Time series of ''nonseasonal variability'' were then obtained by subtracting these low-frequency variations from the NSCAT wind time series at each grid point. To focus on wind variability during the ''jet season'' when cold fronts sweep southeastward across the Inter-American Seas, the analysis was further refined by computing the statistics only over the period December 1996–May 1997. This 6-month period was shown by CFE to correspond to the 1996–97 jet season.

For the Tehuantepec jet (Fig. 4), removal of the seasonal variations decreased the R^2 values slightly but the regions of significant correlation are generally very similar to the case shown in Fig. 1. The relatively small effect of removing the seasonal cycle is not surprising in view of the fact that only about one-sixth of the variability of the Tehuantepec jet was accounted for by seasonal variations.

The most notable impact of removal of the low-frequency seasonal variability is that the correlations of the Tehuantepec jet with wind variations in the vicinity

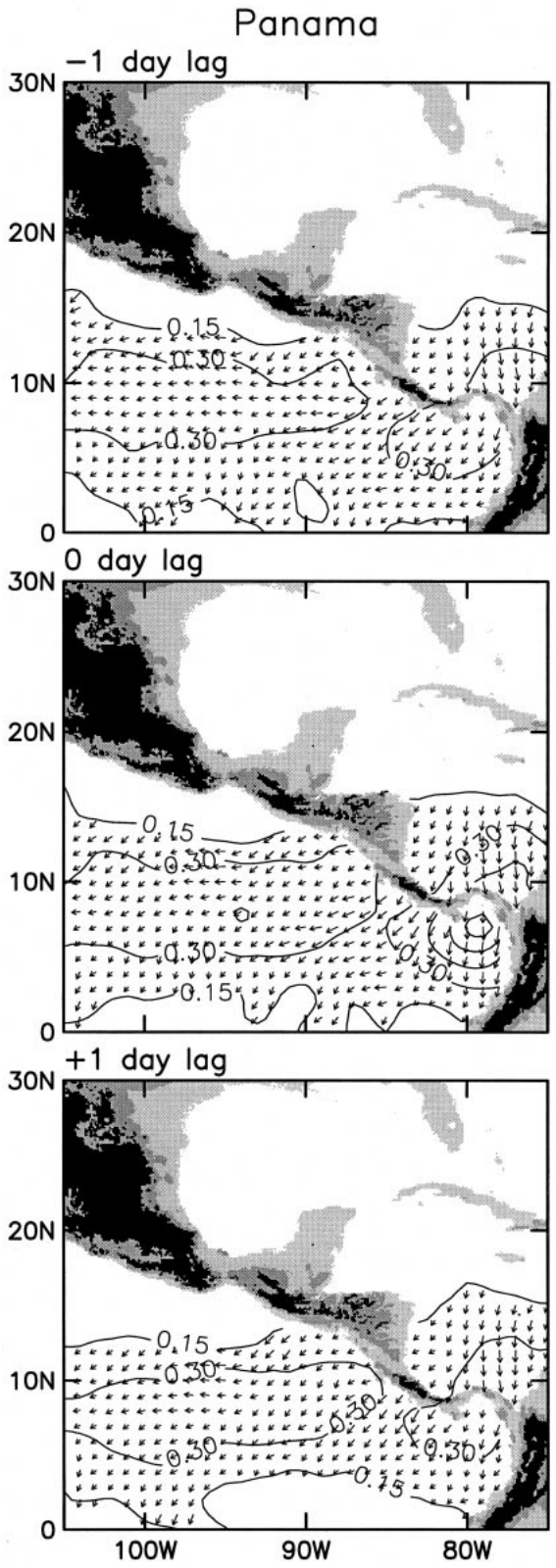

FIG. 3. The same as Fig. 1 except for regressions of the major-axis component of the Panama jet at 7°N, 79°W onto vector winds on a 1° × 1° grid at lags of −1, 0, and +1 days.

of the Papagayo jet improved somewhat at lags of 0 and +1 day. It is noteworthy, however, that the R^2 values in this region decrease eastward and are very small in the immediate vicinity of the Papagayo gap outflow (see especially the zero-lag regression map). In other words, the largest R^2 values occur in the downstream extension of the Papagayo jet. This suggests that the interactions responsible for the apparent link between short-period variability in the Tehuantepec and Papagayo jets may be much more complex than simple generation by southward penetration of cold fronts into the western Caribbean Sea. As suggested in section 3a, the winds induced in the downstream extension of the Papagayo jet may, for example, be generated by airmass adjustments in the eastern tropical Pacific associated with the flow through the Tehuantepec gap. From NSCAT observations alone, it is not possible to deduce the dynamics of the apparent link between the Tehuantepec jet and the downstream extension of the Papagayo jet. The interactions responsible for this feature are best investigated from a mesoscale modeling study such as that carried out by Steenburgh et al. (1998), except with the modeling domain expanded southward to include the Papagayo jet.

It is apparent from Fig. 4 that removal of the seasonal cycle does not improve the correlation between the Tehuantepec jet and the Panama jet. There is no statistically significant relationship between these two jets at any lags. Thus, while the possibility of a link between these two jets is not precluded in specific case studies [e.g., the March 1993 case study described by Schultz et al. (1997), and the December 1996 case study and the early stages of the November 1996 case study described by CFE], some other mechanism must be responsible for most of the variability of the Panama jet.

The impact of removal of the seasonal variations is more significant in the regression maps for the Papagayo and Panama jets (Figs. 5 and 6). In both cases (especially the Panama case), the R^2 values are reduced more than in the Tehuantepec case shown in Fig. 4. Much of the high correlation in Figs. 2 and 3 is therefore attributable to the energetic low-frequency seasonal variability of the Papagayo and Panama jets. Importantly, however, the geographical patterns of the R^2 contours for the nonseasonal variability in Figs. 5 and 6 are very similar to those obtained when the seasonal variations are included in Figs. 2 and 3. In particular, the correlation structures are zonally banded for both jets and the correlations of the Papagayo and Panama jets with nonseasonal variations of the winds over the Gulf of Tehuantepec and Gulf of Mexico are negligible. The R^2 values over these higher-latitude regions do not improve for lags longer than those shown in Figs. 5 and 6.

The fact that removal of the seasonal variability has comparatively little effect on the correlation structure of the Tehuantepec jet but significantly decreases the R^2 values in the correlation structures of the Papagayo and Panama jets underscores the fundamental difference between the relatively short timescales of variability in the

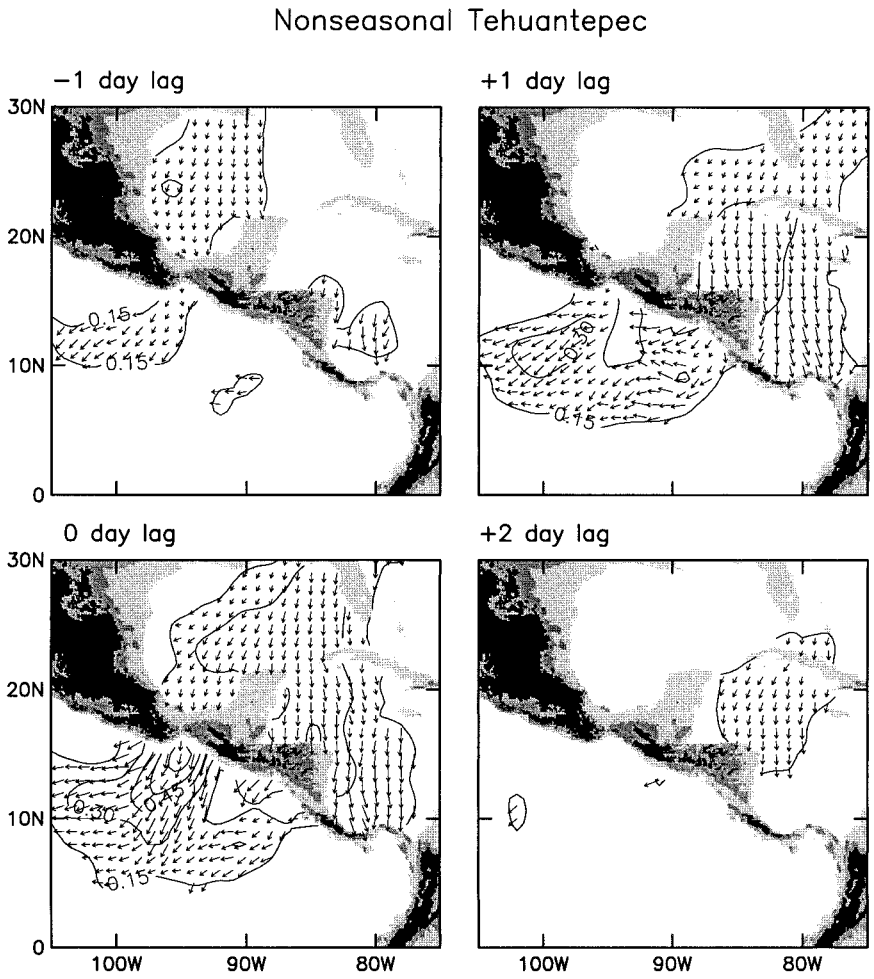

FIG. 4. The same as Fig. 1 for the Tehuantepec jet except for the nonseasonal variations defined to be the deviations of the winds at all locations from least-squares fits to the sum of an annual and a semiannual harmonic. Statistics are computed only over the 6-month jet season Dec 1996–May 1997.

Tehuantepec jet and the longer timescales of variability in the two lower-latitude jets. A perhaps surprising result of the analysis of nonseasonal variability in this section is that, even on short timescales after removal of the low-frequency seasonal variations, continued southeastward movement of the midlatitude high pressure systems that generate Tehuantepec winds evidently accounts for very little of the variability of the Papagayo and Panama jets. Most of the variability of the two lower-latitude jets is associated with zonally coherent trade wind variations on the short nonseasonal timescales as well as on low-frequency seasonal timescales.

4. Pressure forcing of the wind jets

As summarized by Overland and Walter (1981) and Overland (1984) [see also Steenburgh et al. (1998) for a thorough recent review], gap winds are characterized by an approximate along-gap balance between the pressure gradient and inertial accelerations. The throughflow is thus driven by the cross-isthmus pressure differential. In this context, a ''gap'' is considered to be a channel bounded by steep topography with a small ratio of cross-gap to along-gap length scales.

The along-gap pressure gradient forcing mechanism is easily investigated for the three Central American wind jets by correlating the cross-isthmus pressure difference with the major-axis component of the gap outflow at the point where the core of the wind jet leaves the coast. NCEP-reanalyzed 2.5° × 2.5° × 6-h gridded SLP fields (Kalnay et al. 1996) were used to estimate the cross-isthmus pressure gradients at the three gap locations. The mean and standard deviation of the SLP field over the 9-month duration of the NSCAT data record are shown in Fig. 7. It can be seen that both the means and the standard deviations were much larger over the Gulf of Mexico than elsewhere in the region of interest. The mean pressure difference across the Te-

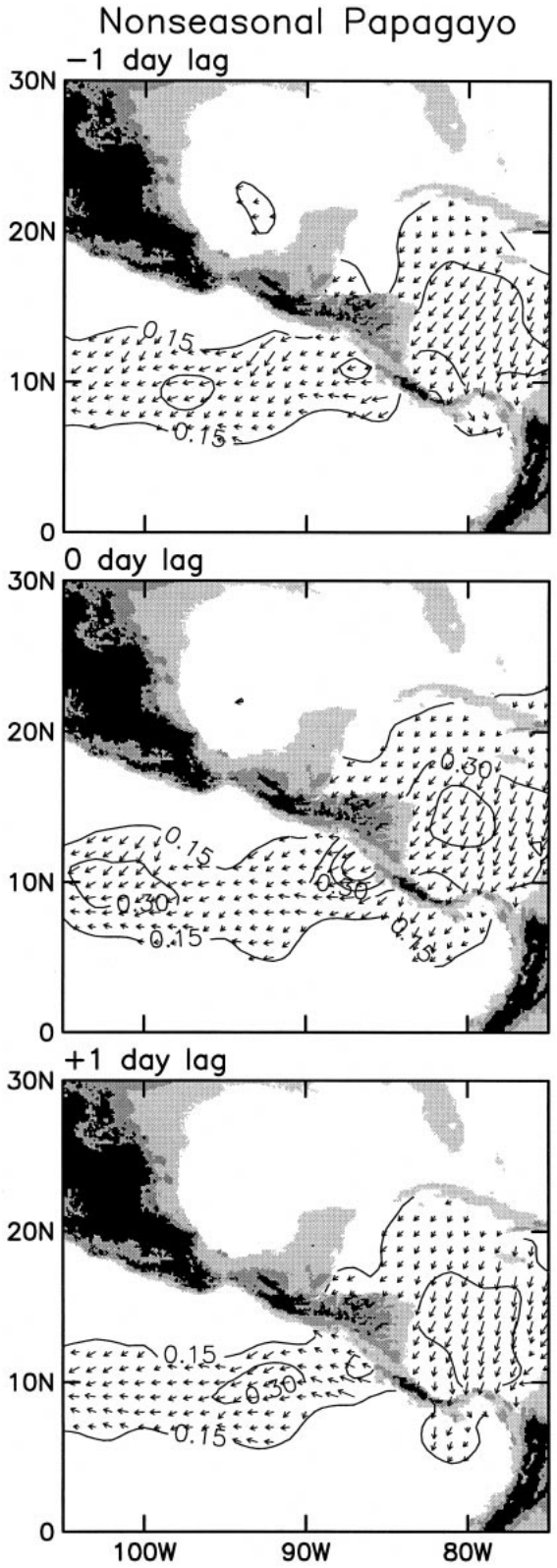

FIG. 5. The same as Fig. 2 for the Papagayo jet except for the nonseasonal variations defined as in Fig. 4 for the period Dec 1996–May 1997.

huantepec gap was about 1 hPa and typical SLP variations were more than 50% larger in the Bay of Campeché (about 4 hPa) than in the Gulf of Tehuantepec (about 2.5 hPa). The across-gap pressure difference can be much larger than this during specific events. For example, Schultz et al. (1997) documented an event that occurred during March 1993 in which the across-gap pressure difference reached 16 hPa.

In contrast with the Tehuantepec gap, the mean pressure difference across Central America was very small at the locations of the Papagayo and Panama gaps and typical SLP variations were only about 2 hPa on both sides of these two gaps. Thus, unlike the Tehuantepec gap for which the across-isthmus pressure differences are clearly dominated by variations in the Gulf of Mexico, it is unclear from the SLP means and standard deviations in Fig. 7 whether pressure variations in the Caribbean play the dominant role in determining the across-gap pressure differences at the locations of the Papagayo and Panama jets.

To quantify the relationships between the intensities of the three gap outflows and along-gap pressure gradients, daily averages of the cross-isthmus pressure differences were computed from the NCEP SLP values at the pair of grid points nearest the two sides of each major gap. These pressure gradient time series were then correlated with the daily average major-axis wind component time series shown in Fig. 13 of CFE. The correlation values computed over the full 9-month NSCAT data record from approximately 190 observations at each location are 0.83, 0.74, and 0.65 for Tehuantepec, Papagayo, and Panama, respectively. The values of N^* for these three locations are 98, 31, and 29 and the corresponding 99% significance levels for the correlations are 0.26, 0.46, and 0.48, respectively. The smaller values of N^* for Papagayo and Panama again reflect the dominance of highly correlated low-frequency variations at these locations. The higher correlation value and much greater statistical significance of the correlation for the Tehuantepec jet emphasizes the dominance of the across-gap pressure gradient mechanism for generation of Tehuantepec winds.

Contour maps of the correlations between the wind jets and the SLP time series at each 2.5° grid point offer further insight into why the Tehuantepec correlation is higher than the Papagayo and Panama correlations. In the maps of the correlations between SLP and the major-axis component of the Tehuantepec wind jet (upper panel of Fig. 8), the correlation contours on the Inter-American Seas side of Central America are roughly concentric about a maximum of about 0.8 over an area immediately upwind (north) of the gap along the western boundary of the Gulf of Mexico. Over the eastern tropical Pacific, the Tehuantepec correlation contours are oriented approximately zonally and decrease rapidly toward the equator; the correlations are less than 0.1 throughout the eastern tropical Pacific equatorward of about 8°N. The correlation patterns on the two sides of the Te-

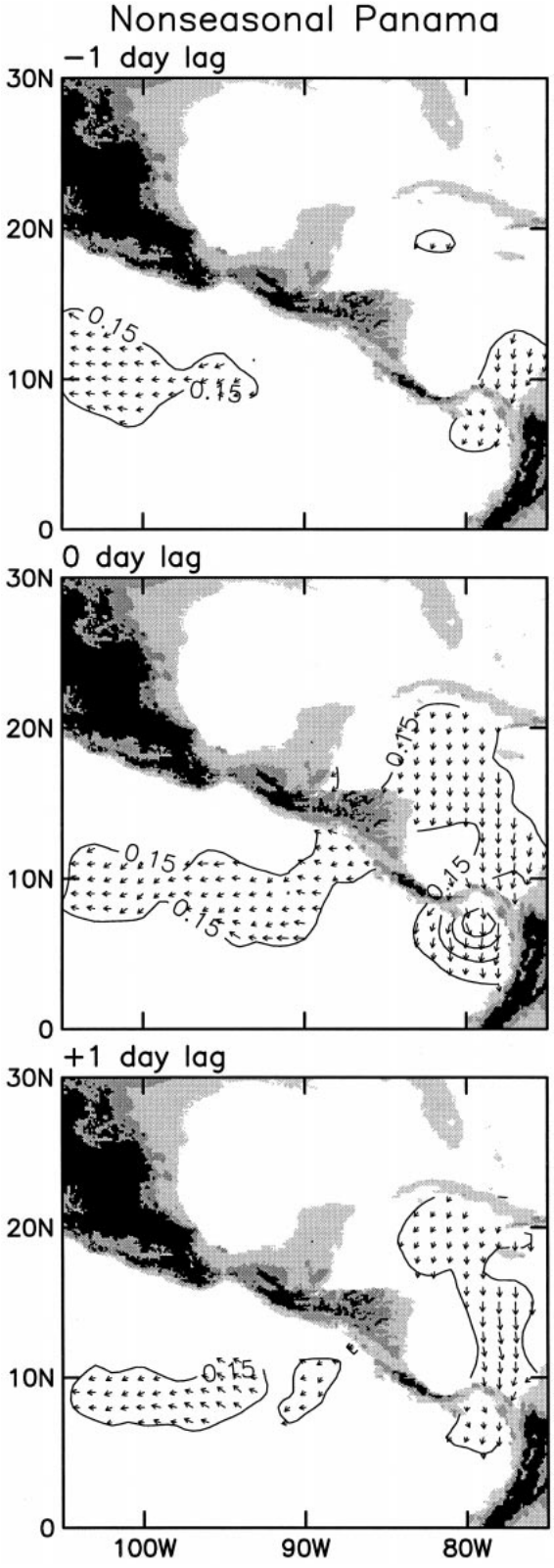

FIG. 6. The same as Fig. 3 for the Panama jet except for the nonseasonal variations defined as in Fig. 4 for the period Dec 1996–May 1997.

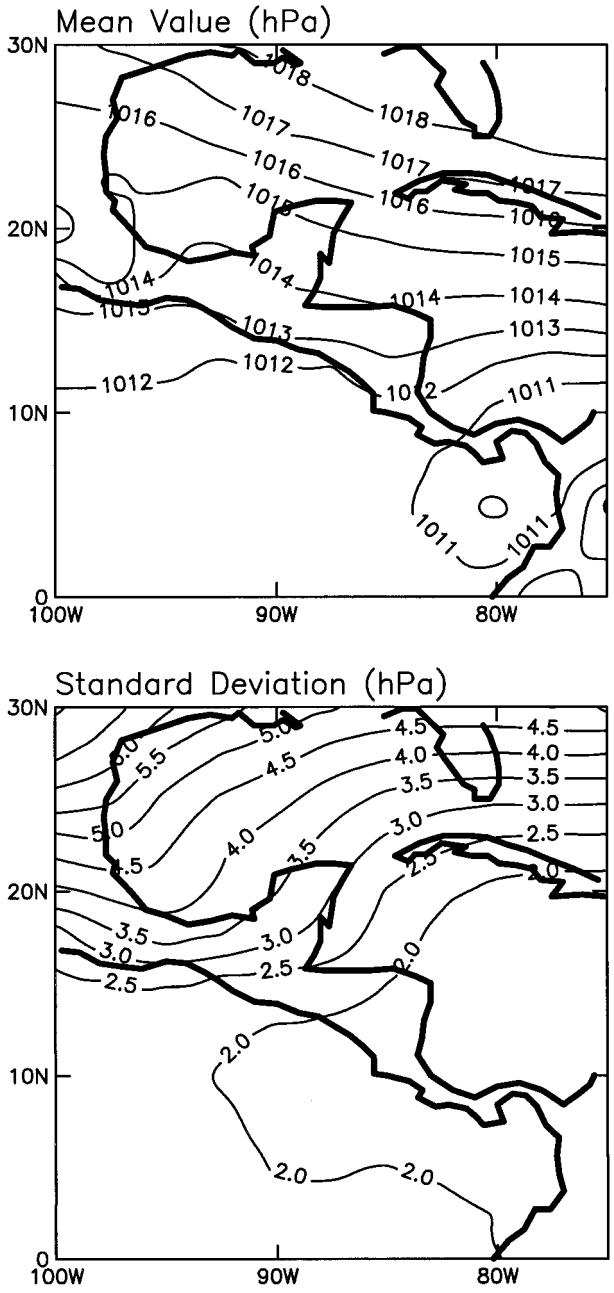

FIG. 7. The mean (top) and standard deviation (bottom) of sea level pressure in hPa computed from the 2.5° × 2.5° × 6-h gridded analyses produced by NCEP.

huantepec gap validate the conclusion that the cross-isthmus pressure gradient that drives the Tehuantepec jet is controlled by pressure variations over the Gulf of Mexico.

The maps of the correlations between SLP and the major-axis components of the Papagayo and Panama wind jets (middle and bottom panels of Fig. 8) are dramatically different from the Tehuantepec correlation map. In particular, there is no localized maximum cor-

relation with SLP on the immediate upwind side of either of these gaps. Indeed, the correlation contours are approximately zonally oriented with negligible correlation magnitudes immediately upwind or downwind of the Papagayo and Panama gaps. The maximum correlations occurred at a much higher latitude than the Papagayo and Panama gaps. The highest correlations were over the northern Caribbean Sea, the eastern Gulf of Mexico and the Straits of Florida. The maximum was located a few degrees farther north for Papagayo than for Panama and the magnitude of the maximum correlation was higher for Papagayo.

The zonal alignment of the correlation contours and the transition from positive correlations over the northern Caribbean Sea to negative correlations over the southern Caribbean Sea are key features of the correlation maps for the Papagayo and Panama jets. The conclusions of section 3 provide a straightforward interpretation of these SLP correlation patterns. It was argued from the correlation structures of the NSCAT wind fields that the Papagayo and Panama wind jets are driven by large-scale variations of the trade winds. To the extent that these trade wind variations are in near-geostrophic balance, this hypothesized link between the Papagayo and Panama jets and the large-scale trade wind field would imply a strong correlation between the jets and the meridional pressure gradient upstream of these two gaps. This speculation is confirmed by the fact that the correlations of the Papagayo and Panama winds with the meridional pressure gradient at 12.5°N, 77.5°W (a crude index of geostrophic trade winds in the Caribbean Sea) are 0.82 and 0.70, respectively.

The zonal banding and latitudinal variations of the signs of the correlations in the Papagayo and Panama maps in Fig. 8 are thus fully consistent with a link between these two wind jets and the trade winds that span Central America from the Caribbean to the Pacific. The latitude of the maximum meridional gradient of the correlation values is slightly lower for Panama than for Papagayo. This is consistent with the regression maps in Figs. 3 and 6 that suggest that Panama winds are coupled to equatorward shifts of the axes of the Caribbean and Pacific trade winds.

5. Structures of the wind jets

Although the NSCAT data provide unprecedented spatial and temporal coverage of the structure of surface winds, measurements of other dynamically important variables (e.g., atmospheric pressure and the vertical structure of the turbulent boundary layer) are not available on the spatial scales resolvable by NSCAT winds to allow detailed analyses of the force balances in the jets. The NSCAT data are nonetheless useful for interpreting previously published observations and models of the jets. These previous studies have focused almost entirely on the Tehuantepec jet, presumably because it is by far the most energetic of the three jets (see Fig.

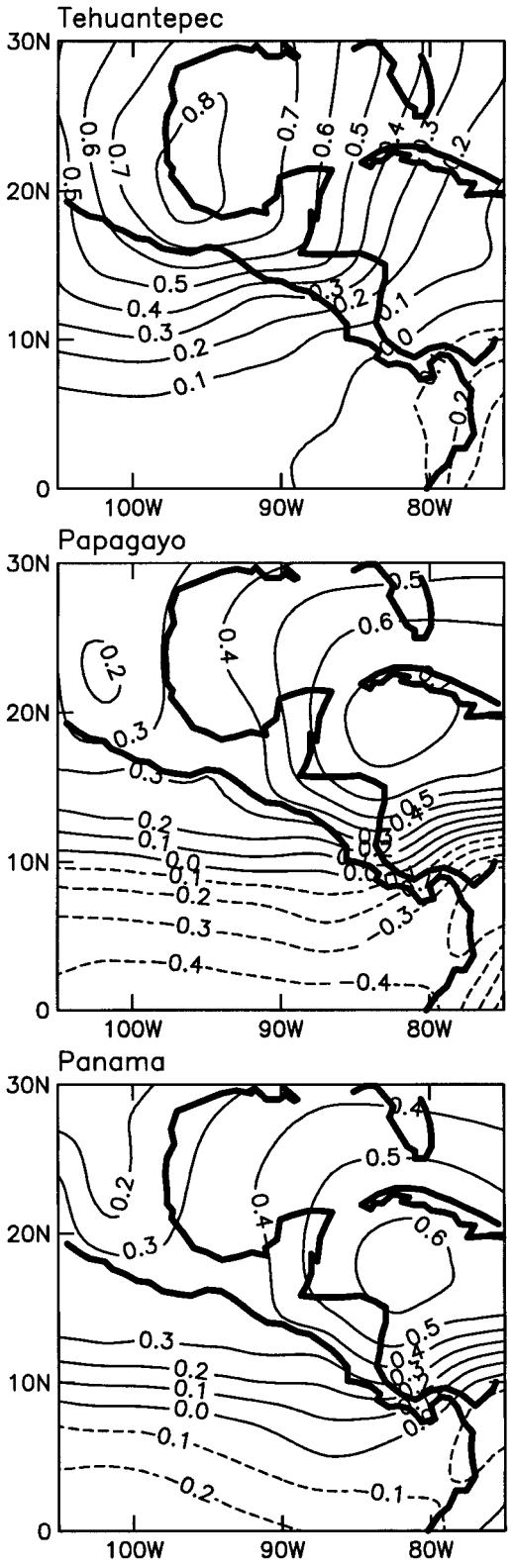

FIG. 8. Maps of the correlations between the three wind jet major-axis wind component time series shown in Fig. 13 of CFE and daily averaged 2.5° × 2.5° × 6-h analyses of sea level pressure over the domain of interest.

11b of CFE) and because of the almost complete lack of direct observations of the Papagayo and Panama jets. A historical summary of previous observations of the structure of the Tehuantepec jet is presented in section 5a. The structures of each of the three jets inferred from the NSCAT observations are then summarized in sections 5b–d.

a. Historical observations of the Tehuantepec jet

It has long been known that the Tehuantepec winds extend far into the Pacific Ocean. Because of the sparse wind observations available offshore, however, the detailed structure of the jet after it leaves the coast and blows over the Gulf of Tehuantepec is only now becoming clear. Hurd (1929) noted that the Tehuantepec winds spread hundreds of kilometers into the Pacific and that the wind directions were considerably variable in the lower reaches of the Gulf of Tehuantepec. But there is no indication that he was aware that the winds turn anticyclonically toward the west over the gulf. Parmenter's (1970) analysis of a single Tehuantepec wind event from satellite cloud images showed a squall line that was interpreted as the forward edge of cold air in the gap outflow. The squall line started as a fairly symmetric arc over the northern gulf. As time progressed, the arc cloud dissipated on the eastern side and moved quickly westward. It is unclear whether Parmenter recognized this as evidence of anticyclonic turning of the axis of maximum winds.

The first comprehensive attempt to synthesize a picture of the surface wind field over the Gulf of Tehuantepec was an analysis of merchant ship observations by Roden (1961). Although he concluded that the quality of these historical data was only moderate, he was able to show that the winds decreased rapidly east and west of the jet axis. Seaward of the coast, however, the wind speed decreased slowly and the jet extended several hundred kilometers to the south. Roden interpreted the line of zero wind stress curl as the axis of the Tehuantepec jet. The zero contour in his map of February wind stress curl exhibited a very slight anticyclonic curvature, but not enough to suggest any significant turning of the Tehuantepec wind jet.

Clarke (1988) appears to have been the first to suggest that the Tehuantepec wind jet turns anticyclonically westward after leaving the coast. His evidence was indirect, however, based on satellite measurements of SST that showed a cold tongue of water that formed almost immediately after the onset of a Tehuantepec wind event in January 1986. The minimum SST in this cold tongue extended southward from the coast and then turned westward along 12.5°N. Clarke argued that the sudden appearance of cold water must have been induced by wind mixing along the path of the wind jet. The curved pattern of minimum SST was therefore interpreted as coincident with the path of the wind jet.

The baroclinic Rossby radius of deformation for a two-layer approximation of the atmospheric circulation is

$$L = \frac{\sqrt{g'H_1}}{f},$$

where H_1 is the mixed-layer depth, $f = 2\Omega \sin\phi$ is the Coriolis parameter for Earth rotation rate $\Omega = 7.29 \times 10^{-5}$ s^{-1} and latitude ϕ, and $g' = g(\theta_2 - \theta_1)/\theta_1$ is the reduced gravity for gravitational acceleration $g = 9.8$ m s^{-2} and lower- and upper-layer potential temperatures of θ_1 and θ_2, respectively. An estimate of L can be constructed based on the model simulation of a Tehuantepec wind event by Steenburgh et al. (1998). From their Figs. 10 and 11, the boundary layer thickness is $H_1 \approx 2000$ m and the potential temperatures are $\theta_1 \approx 296$ K and $\theta_2 \approx 304$ K. For the value of $f = 3.8 \times 10^{-5}$ s^{-1} appropriate for latitude 15°N, the baroclinic Rossby radius is $L \approx 600$ km. The ~40 km width of the Tehuantepec gap is therefore more than an order of magnitude smaller than the Rossby radius. From a scale analysis, Clarke (1988) thus proposed a model of the outflow as a narrow inertially balanced jet.

The path of a wind jet for purely inertial motion is easily determined from the force balance on an air parcel. The cross-stream pressure gradient is negligible within the jet and the Coriolis force is balanced by the centrifugal force. The trajectory of an air parcel with wind speed v can easily be shown to be a circle with radius

$$r = \frac{v}{f}$$

(see, e.g., Clarke 1988; Holton 1992, p. 64). Clarke showed that the curvature of the cold tongue of water was consistent with the anticyclonic turning of an inertial path for a gap outflow of 15.3 m s^{-1}.

Schultz et al. (1997) recently presented additional indirect evidence in support of Clarke's (1988) hypothesis that the Tehuantepec wind jet follows an inertial path after leaving the coast. Satellite observations showed the leading edge of the gap outflow during a major Tehuantepec wind event in March 1993 to be marked by an arc-shaped line of cumulus convection resembling a rope cloud, presumably oriented perpendicular to the wind direction. In a manner qualitatively consistent with a wind jet following an inertial trajectory, isochrones of the rope cloud turned anticyclonically toward the west. From the limited direct wind observations available at the time of the cloud observations it was not possible to determine whether an inertial balance was quantitatively valid. However, Schultz et al. (1997) showed that the 1° × 1° gridded analyses of 10-m winds by the European Centre for Medium-Range Weather Forecasts (ECMWF) for the time period of interest turned anticyclonically to the west along a path that was at least qualitatively consistent with an inertial path.

The only attempt that we are aware of to construct a

picture of the detailed structure of the surface wind field within the jet from direct observations over a broad area of the Gulf of Tehuantepec is reported in a pair of papers by Barton et al. (1993) and Trasviña et al. (1995). They presented a 3-week composite average map of surface wind observations from a pair of ships that surveyed the oceanographic and meteorological conditions during a moderate Tehuantepec wind event in late January 1989. Despite the limitations of a 3-week composite average during a period when the wind strength changed considerably, the anticyclonic turning of the wind jet is clearly evident along the southernmost ship track in their survey. Their wind observations also reveal a symmetric off-axis fanning of the wind jet away from the head of the gulf. They suggested that this fanning contradicted Clarke's (1988) model of the gap outflow as a narrow inertial jet. The fan-shaped pattern on the edges of the jet evidently indicates a cross-flow component of force away from the axis of the jet.

Because of the difficulty in acquiring high-resolution surface wind measurements with broad areal coverage over the Gulf of Tehuantepec, the most detailed description of a Tehuantepec wind jet that is available to date was developed from a model simulation. The March 1993 Tehuantepec event discussed by Schultz et al. (1997) has recently been simulated by Steenburgh et al. (1998) using the high-resolution Pennsylvania State University–National Center for Atmospheric Research mesoscale model MM5. The model simulation produced an off-axis fanning of the gap outflow similar to the January 1989 event described by Barton et al. (1993) and Trasviña et al. (1995). The winds were strongly anticyclonic to the west of the jet axis and less anticyclonic to the east.

From a careful analysis of the cross-flow momentum balance along Lagrangian trajectories in their simulation, Steenburgh et al. (1998) concluded that the axis of the jet was in almost perfect inertial balance over the distance considered in their analysis. The radii of curvature for trajectories close to the jet axis closely matched those of an inertial path for the gap outflow of 22 m s^{-1}. The most southerly point considered was at a latitude of about 14.2°, which is about 200 km from the coast. The Steenburgh et al. analysis thus indicates that the jet axis in the model maintained an inertial trajectory over at least this distance.

Away from the jet axis, the Lagrangian trajectories in the model did not follow inertial paths. Trajectories on the west side of the jet had stronger anticyclonic curvature (smaller radii of curvature) than inertial trajectories. The opposite was true on the east side of the jet where trajectories were very nearly straight southward. The momentum balances on the sides of the jet axis indicated that the off-axis fanning of the jet was caused by a strong cross-flow pressure gradient away from the jet axis. The opposing pressure gradients on opposite sides of the model jet axis were established by a mesoscale pressure ridge that developed along the jet axis from the southward advection of cold air of higher-latitude origin. On the west side of the jet, the model pressure gradient augmented the Coriolis acceleration, resulting in a trajectory with stronger anticyclonic curvature than the inertial path along the axis. On the east side of the jet, the pressure gradient opposed the Coriolis acceleration, resulting in less curvature than along the jet axis.

A noteworthy inconsistency between the Tehuantepec winds simulated by Steenburgh et al. (1998) and the observations by Barton et al. (1993) and Trasviña et al. (1995) is a distinct difference in the wind directions on the east side of the jet axis. The observed winds had a much stronger westerly component than the model winds. In fact, the model winds had virtually no westerly component at all. The significance of this discrepancy in the off-axis fanning east of the jet axis is difficult to judge because the observations and model simulation are for two different wind events separated by four years. In addition, composite averaging over 3 weeks was necessary to construct the map of the January 1989 wind field from the ship observations; it is conceivable that the greater observed westerly component in this event could be an artifact of the nonsynopticity of the observations. One of the objectives of this study is to investigate the detailed structure of the Tehuantepec wind jet from the NSCAT observations and thus assess the validity and significance of the more extensive off-axis fanning of the jet suggested by the ship observations on the east side of the jet axis.

b. NSCAT observations of the Tehuantepec jet

The structure of the surface wind field over the Gulf of Tehuantepec is clearly depicted in the 2-day composite maps constructed from NSCAT data for the case studies described by CFE. Except during the influence of tropical storm Marco in the late stages of the November case study, the cores of the Tehuantepec jets in all three case studies turned anticyclonically to the west and winds fanned outward from the core of the jet. As noted previously by CFE from the 9-month vector-average wind field and the alignment of the major axes of the velocity variance ellipses, the anticyclonic turning and fanning are persistent features of the Tehuantepec jet. In this section, we quantitatively test the notion that the observed paths of the Tehuantepec jets are consistent with those of inertial jets over the wide range of jet intensities observed during the 9-month NSCAT data record. We also investigate the structure of the off-axis fanning of the jet and relate the observations to the modeling results of Steenburgh et al. (1998).

A purely inertial jet implies circular motion from the centrifugal force that balances the Coriolis force on an air parcel exiting the gap. The addition of frictional forces would retard the wind velocity, resulting in a spiral trajectory with a radius of curvature that decreases with increasing distance from the gap (e.g., Clarke

1988). This theoretical inward spiral is in stark contrast to the NSCAT observations; the radius of curvature of the core of the jet consistently increased with increasing distance from the gap, ultimately becoming approximately zonal along 10°N (effectively equivalent to an infinite radius).

Simple dynamical considerations indicate that geostrophic adjustment of the wind jet should occur over a distance of the order of the Rossby radius of deformation (about 600 km over the Gulf of Tehuantepec, as noted in section 5a). For a gap outflow of 15 m s^{-1}, the radius of an inertial circle at 15°N is $r = 400$ km. An arc length of 600 km along this inertial circle corresponds to an anticyclonic turning of 86°. The Tehuantepec jet would therefore come into geostrophic equilibrium after about a quarter revolution of an inertial circle. A cross-stream pressure gradient force must develop along the trajectory toward the left of the direction of motion (in opposition to the Coriolis force) so that a near-geostrophic balance is established by the time the gap outflow becomes an easterly jet. Near the coast, the gap outflow cannot be purely inertially balanced off the axis of the jet since lateral turbulent mixing introduces additional accelerations. Nonetheless, it is not unreasonable to hypothesize that the axis of the jet is inertially balanced sufficiently close to the gap.

A rigorous test of the validity of the inertial balance along the axis of the wind jet has not been possible from previous observations since measurements have not been available with sufficient spatial and temporal coverage over the Gulf of Tehuantepec. The approach used here to investigate the possibility of an inertial balance was to determine an inertial path based on each 2-day composite average NSCAT measurement of the speed of the gap outflow. The predicted wind direction was then compared with the observed wind direction at several points along the inertial path.

Because the NSCAT data coverage decreases near the coast owing to land contamination in the radar footprints, a reference location for the speed of the gap outflow was defined to be 15.25°N, 95°W, which is far away from any possibility of land contamination of the radar return. The NSCAT measurements of wind direction at this location were very consistent, averaging about 10° clockwise from north (Fig. 9). Since this reference location is about 75 km south of the coast, some anticyclonic turning is to be expected if the jet is in inertial balance at the gap. Because the reduction of wind speed from frictional effects is small over this short distance, it is reasonable to calculate the radius of an inertial circle based on the wind speed at the reference location. The inertial path for this wind speed was then defined by assuming a wind direction of 0° (northerly) at the gap location of 15.75°N, allowing a geometrical determination of the predicted wind direction at any latitude along the inertial path.

The NSCAT observations of wind directions are shown in Fig. 10 at three latitudes along inertial paths

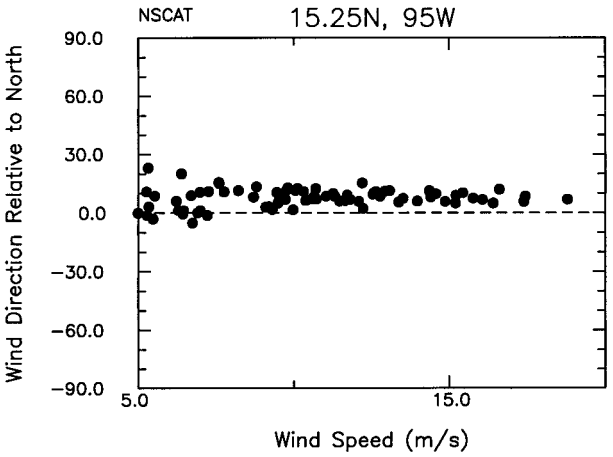

FIG. 9. NSCAT observations of wind direction (clockwise relative to north) as a function of wind speed at the location 15.25°N, 95°W used as a reference for NSCAT estimates of the wind speed of the Tehuantepec gap outflow.

defined as described above, based on the observed wind speeds at the reference location. The solid lines represent the predicted wind direction for an inertial jet as a function of wind speed for wind speeds in excess of 5 m s^{-1}, which usually constitute a well-defined jet. At wind speeds below about 13 m s^{-1} there is considerable scatter of the observed wind directions. The scatter decreases at higher wind speeds. At all wind speeds, there are very few cases for which the observed wind direction was larger (more clockwise from north) than the predicted wind direction; the predicted wind direction thus constitutes a well-defined upper bound on the distribution of observed wind directions at all three latitudes. The observed anticyclonic turning of the Tehuantepec jets after they leave the coast is thus almost always less than or equal to the predicted turning of a purely inertial jet.

The smaller discrepancies between the predicted and observed wind directions at the highest latitude considered here (top panel of Fig. 10) has implications for the validity of the inertial balance. For gap outflows higher than about 13 m s^{-1}, the observed wind directions are indistinguishable from the wind direction of a purely inertial jet. At the two more southerly latitudes farther from the coast (middle and bottom panels of Fig. 10), the discrepancies between predicted and observed wind directions increase. This would occur if some lateral force develops in opposition to the Coriolis force, thus causing the winds to veer less anticyclonically than a purely inertial jet. Dynamically, the geostrophic adjustment of large-scale flows results in a cross-stream pressure gradient force that develops in opposition to the Coriolis force soon after the jet leaves the coast. A near-geostrophic balance is established over a distance comparable to the ~600 km Rossby radius of deformation.

These comparisons between observations and theory

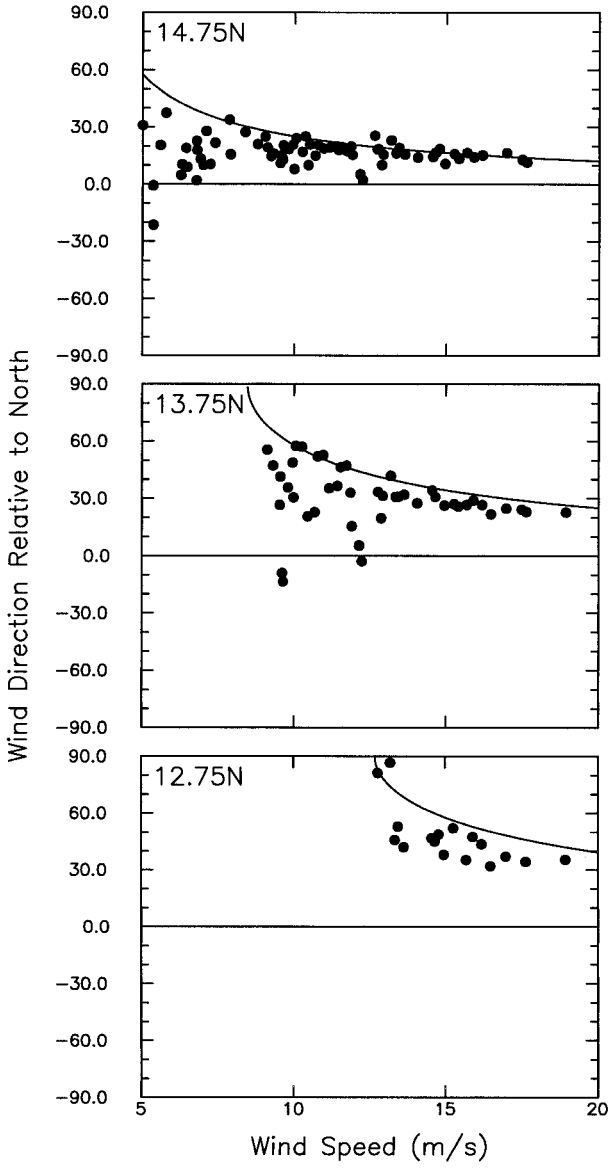

FIG. 10. Predicted wind directions for inertial jets (curved lines) and observed wind directions (dots) as a function of the speed of the Tehuantepec jet at the gap opening. Wind speeds and directions were determined from 2-day composite average maps at the intersections of latitudes 14.75°N, 13.75°, and 12.75°N with inertial paths originating at the gap opening with the observed wind speed at 15.25°N, 95°W and an initial northerly direction.

must take into account the fact noted by CFE that the spatially averaged NSCAT wind measurements can underestimate the wind speed in regions of strong horizontal gradients such as those near the cores of the Tehuantepec wind jets. The effects of this spatial smoothing are difficult to quantify since the bias, if it exists, is not known. The discrepancy between the observed and predicted wind directions can be almost entirely accounted for if the NSCAT spatially averaged wind speeds are biased low by 20%, which is probably an upper bound on the actual value. However, frictional forces will decrease the wind speed with increasing distance along the axis of the jet [see Fig. 16 of Steenburgh et al. (1998)]. It can be seen from Figs. 11 and 12 below that the wind speed decreases by more than 20% between the coast and the 12.75°N latitude shown in the bottom panel of Fig. 10. This decrease in the wind speed would completely offset any bias from NSCAT underestimates of the speed of the gap outflow.

We therefore conclude that the anticyclonic turning of the Tehuantepec wind jet at the two most southerly latitudes considered in Fig. 10 is generally less than the predicted turning of an inertial jet. This is consistent with the dynamical notion that the forces on an air parcel in the core of the wind jet are in inertial balance at the gap outflow and adjust toward a geostrophic balance with increasing distance from the gap.

Investigation of the off-axis fanning of the Tehuantepec wind jet after it leaves the coast yields additional insight into the dynamical balances within the jet. As noted previously in section 5a, a composite average of three weeks of ship observations by Barton et al. (1993) and Trasviña et al. (1995) suggested a divergent fanning of the jet that is considerably stronger than the fanning in the model simulation of a different event by Steenburgh et al. (1998). From the case studies presented by CFE, the stronger fanning deduced from the ship observations is much more representative of the wind field observed by NSCAT.

An enlargement of the Gulf of Tehuantepec region for the 2-day period 19–20 December 1996 during the December case study described by CFE is shown in the upper-left panel of Fig. 11. The association of this wind event with high SLP in the Gulf of Mexico is shown in Fig. 4 of CFE. The divergence and relative vorticity of this 2-day composite average wind field are shown on the left in the middle and bottom panels, respectively. The jet was strongly divergent in the upper reaches of the gulf with small areas of convergent flow near the coast on the east and west sides of the jet. The concentration of the flow in the core of the jet is evident by the consistently positive relative vorticity east of the jet axis and the consistently negative relative vorticity west of the jet axis.

For comparison, the 2-day composite average of 1° × 1° × 6-h gridded ECMWF analyses[3] of 10-m winds is shown in the upper-right panel of Fig. 11. To avoid interpretational difficulties owing to possible NSCAT

[3] While the 2.5° × 2.5° gridded NCEP analyses of SLP and 10-m winds presented in section 3 of CFE and analyzed in section 4 of this study were adequate for the purposes for which they were used, this coarse resolution is clearly inadequate to resolve the spatial structures of the three wind jets of interest here. We were unable to obtain NCEP winds with higher grid resolution. The 1° × 1° gridded analyses of 10-m winds (but not SLP) were made available by ECMWF. We have therefore switched from NCEP to the 1° × 1° gridded ECMWF analyses in this section.

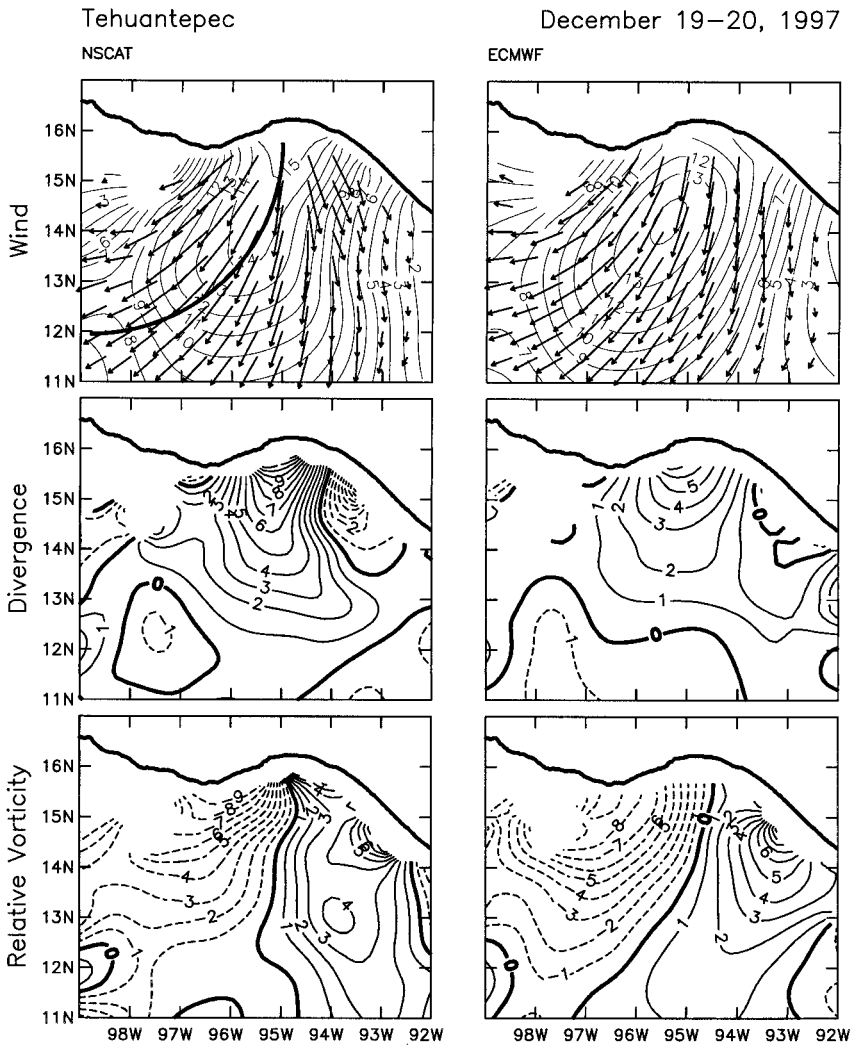

FIG. 11. Composite averages of the 10-m vector wind field (upper), wind divergence (middle), and relative vorticity (bottom) over the Gulf of Tehuantepec for the 2-day period 19–20 Dec 1996. (left panels) Constructed from 2-day composite averages of NSCAT observations over 1° × 1° areas. (right panels) Constructed from 6-hourly 1° × 1° ECMWF analyses of 10-m winds interpolated to the same times and locations as the NSCAT observations and then composite averaged in the same manner as the NSCAT observations. For display purposes, the 1°-averaged NSCAT and ECMWF vector wind fields in the top panels have been spatially interpolated onto a 0.5° grid. The contours in the top panels are the magnitude of the 2-day vector-average winds and the heavy line in the upper-left panel is the inertial path originating at the gap opening with the observed wind speed at 15.25°N, 95°W and a northerly direction.

sampling errors, this wind field was constructed by trilinear interpolation of the 1° × 1° × 6-h gridded ECMWF winds to the same times and locations as the NSCAT observations. Overall, the ECMWF analyses of this event are qualitatively quite good. The underestimation of the wind speed and the offshore displacement of the maximum intensity of the jet are characteristic features of the ECMWF analyses over the 9-month duration of the NSCAT data record.

The most striking difference between the NSCAT and ECMWF wind fields is the much stronger westerly component in the NSCAT winds on the east side of the jet. In fact, there is no westerly component on the east side of the jet axis in the ECMWF wind field. As a consequence of the discrepancy between the off-axis fanning of the jet in the NSCAT observations and ECMWF analyses, the wind jet is much less divergent in the ECMWF wind field (middle panels of Fig. 11). The NSCAT and ECMWF relative vorticity fields also differ significantly on the east side of the jet (see bottom panels of Fig. 11). In comparison, the relative vorticity fields are more similar on the west side of the jet.

Enlargements of the Gulf of Tehuantepec region during the November 1996 and March 1997 case studies

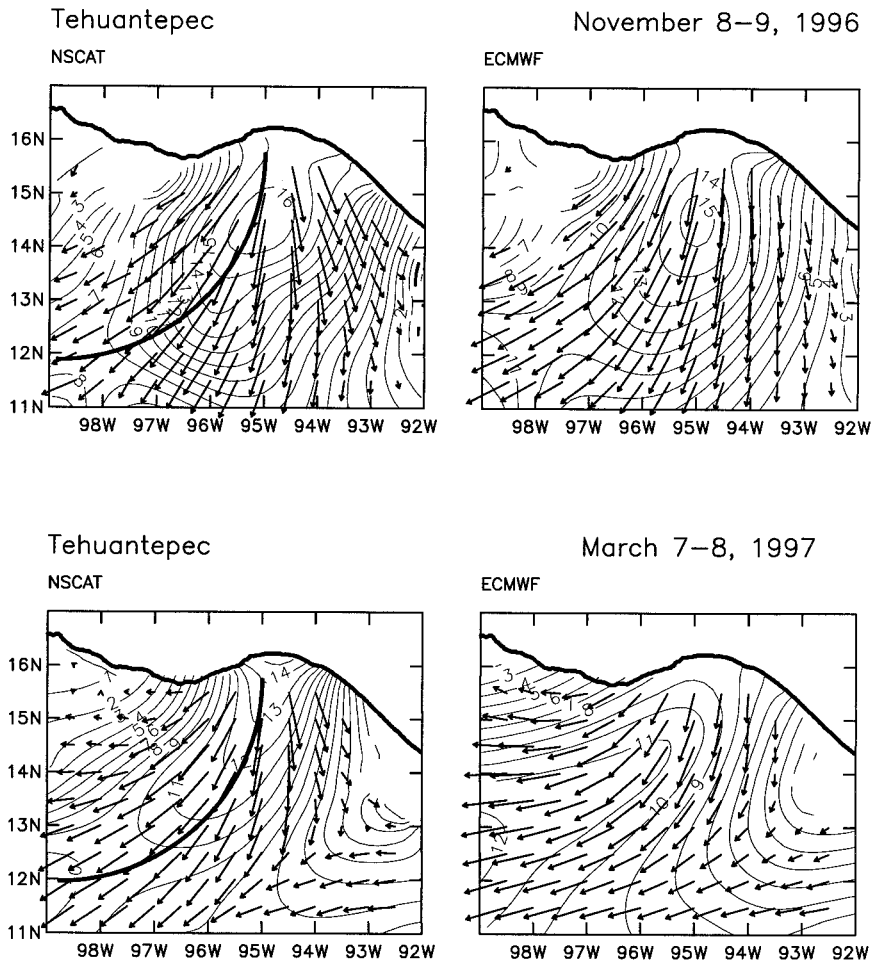

FIG. 12. Composite averages of the 10-m wind field over the Gulf of Tehuantepec for the 2-day periods (top panels) 8–9 Nov 1996 and (bottom panels) 7–8 Mar 1997 constructed from (left panels) NSCAT data and (right panels) ECMWF analyses of 10-m winds as described in Fig. 11. The contours are the magnitude of the 2-day vector-average winds and the heavy lines in the left panels are inertial paths originating at the gap opening with the observed wind speeds at 15.25°N, 95°W, and a northerly direction.

described in sections 3b and 3c of CFE are shown in Fig. 12. The wind divergence and relative vorticity fields (not shown) were similar to the December example in Fig. 11. As in the December example, the NSCAT winds in the November and March examples had large westerly components on the east side of the jet. Also similar to the December example, the ECMWF winds on the east side of the jet had only a weak westerly component during the 2-day period 8–9 November and no westerly component at all during the 2-day period 7–8 March.

The discrepancies between the NSCAT and ECMWF wind directions on the east side of the Tehuantepec jet in the three examples considered above are a general feature over the 9-month NSCAT data record. This is summarized in Fig. 13, which shows the NSCAT and ECMWF wind directions at a location 1° east of the jet axis at 15°N, which is about 100 km south of the gap outflow. The ECMWF wind directions cluster tightly around 0° (northerly). While there is more directional variability at low to moderate wind speeds, the NSCAT wind directions on the east side of the jet axis are almost always more westerly than the ECMWF wind directions, clustering about 27° counterclockwise from north.

Although less consistent than on the east side of the jet, there are systematic differences between the NSCAT and ECMWF wind directions on the west side of the jet as well. As shown in Fig. 14, the NSCAT wind directions west of the jet axis are more variable than the ECMWF wind directions. With increasing wind speed, the wind generally becomes more easterly in the NSCAT data but more northerly in the ECMWF analyses. At wind speeds higher than about 14 m s^{-1}, the NSCAT wind directions cluster around 45° while the ECMWF wind directions cluster about 30°. The ECMWF wind directions at high wind speeds are thus consistently more northerly than the NSCAT observa-

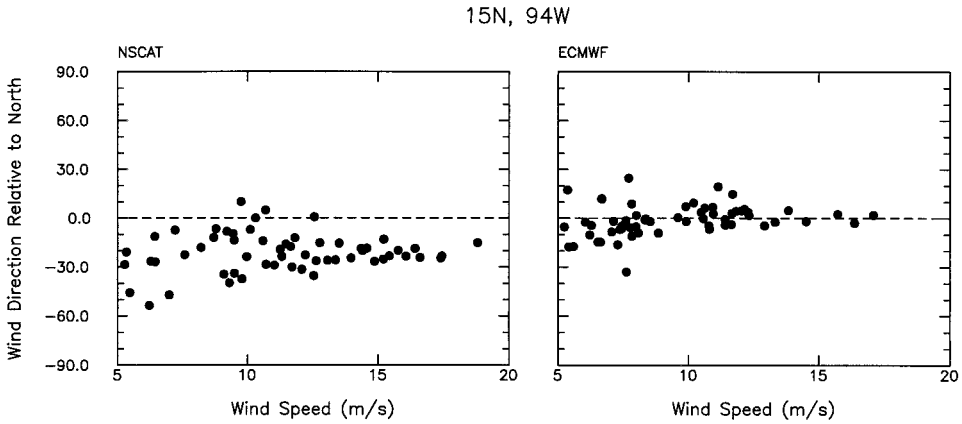

FIG. 13. The wind directions (clockwise relative to north) on the east side of the Tehuantepec wind jet at 15°N, 94°W, shown as a function of the speed of the jet at the gap opening. Wind speeds and directions were obtained from 2-day composite average maps constructed from (left) the NSCAT observations and (right) the ECMWF analyses interpolated to the times and locations of the NSCAT observations.

tions on the west side of the jet axis. The fanning of strong wind jets is therefore also generally weaker on the west side of the jet axis in the ECMWF wind fields.

The weak fanning of the jet in the ECMWF analyses is almost identical to the weak fanning in the mesoscale model simulation of a March 1993 Tehuantepec wind event by Steenburgh et al. (1998). The detailed analysis of the momentum balance by Steenburgh et al. may therefore provide insight into the reason for the weak fanning on the east side of the jets in the ECMWF analyses. They determined the force balance along three Lagrangian trajectories in a jet with gap outflow of 22 m s^{-1}. Along a trajectory that corresponded to the axis of the jet, they found a zero cross-flow pressure gradient and near-perfect inertial balance in the upper reaches of the gulf within 200 km of the coast considered in their analysis. This is consistent with the results in the top panel of Fig. 10.

Because of the high degree of scatter in the relationships between the NSCAT and ECMWF wind directions on the west side of the jet axis, it is difficult to relate the NSCAT observations to the analysis of the momentum balance by Steenburgh et al. However, on the east side of the jet axis where the wind directions in the NSCAT observations and ECMWF analyses are systematically different, the Lagrangian trajectory of an air parcel in the Steenburgh et al. model was almost due southward, as in the winds east of the jet axis in the ECMWF analyses in Figs. 11 and 12. The force balances responsible for the weak fanning in the Steenburgh et al. model may therefore be similar to the force balances on the east side of the jet in the ECMWF analyses. Along the trajectory analyzed by Steenburgh et al., the cross-flow pressure gradient force exceeded the Coriolis force in the model simulation. The precise nature of the westward residual force required to balance the forces on the parcel was not explicitly identified by Steenburgh et al., except to state that it was a combination of diffusion, the parameterized boundary-layer processes in the model, and numerical truncation error.

The consistently greater degree of fanning of the winds on the east side of the jet in the NSCAT observations implies that there is too much westward accel-

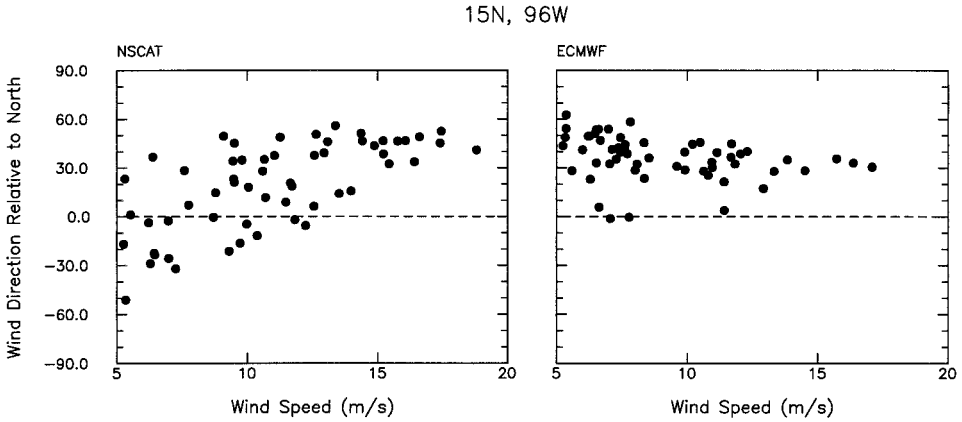

FIG. 14. The same as Fig. 13 except at 15°N, 96°W on the west side of the Tehuantepec wind jet.

eration in the mesoscale model and the ECMWF ''first-guess'' fields in this data-sparse region. This could arise either from an insufficient eastward pressure gradient or an excessive westward residual force. The latter might be an indication of systematic errors in model parameterizations of boundary layer processes. In any case, it is highly unlikely that the stronger fanning on the east side of the jet in the NSCAT observations could be attributed to systematic errors in the NSCAT winds. It is much more likely indicative of errors in the Steenburgh et al. simulation and the ECMWF analyses.

c. NSCAT observations of the Panama jet

An examination of the Panama wind events during the 9-month NSCAT data record reveals that the wind field over the upper reaches of the Gulf of Panama (within a few hundred kilometers of the coast) often shows characteristics similar to the Tehuantepec wind jet. In particular, the core of the jet tends to turn anticyclonically toward the west, suggesting that the jet may be in inertial balance at the gap. The winds also fan away from the axis of the jet as in the Tehuantepec examples considered in section 5b. Because the wind speeds are low in the Panama jet (seldom exceeding 8 m s^{-1}, see CFE), the anticyclonic turning is easily disrupted by other meteorological phenomena unrelated to the gap outflow. This is especially true in the southern reaches of the gulf where the anticyclonic turning of the Panama wind jet can be altered by the southwesterly cross-equatorial flow often found in the eastern tropical Pacific.

An enlargement of the Gulf of Panama region during a particularly clear example of the Panama wind jet at a time when there was no cross-equatorial flow is shown in Fig. 15. The map of the surface vector wind field in the upper-left panel and the corresponding maps of the divergence and relative vorticity fields in the middle and bottom panels were constructed from NSCAT observations over the 2-day period 9–10 March 1997 during the March case study described by CFE. For this event, the characteristics of the Panama jet are very similar to those of the Tehuantepec examples shown in Figs. 11 and 12. The Panama jet turned anticyclonically to the west with a radius of curvature larger than the inertial path and there was a strongly divergent fanning of the jet in the upper reaches of the Gulf of Panama.

The ECMWF analyses of this event are shown in the right panels of Fig. 15. As in the Tehuantepec examples in section 5b, the divergent fanning of the Panama jet during this event was much weaker in the ECMWF wind fields. The relative vorticity (bottom panels of Fig. 15) is similar on the east side of the jet axis in the NSCAT and ECMWF wind fields. On the west side, however, the anticyclonic turning of the jet is much stronger in the NSCAT observations.

d. NSCAT observations of the Papagayo jet

The characteristics of the Papagayo jet were fundamentally different from the Tehuantepec and Panama wind jets. The core of the Papagayo jet never turned anticyclonically to the north during the 9-month NSCAT data record. The inertial balance evidently plays no significant role in the dynamics of the Papagayo gap outflow. This may be an indication that the gap through the Nicaraguan lake district is sufficiently wide that a near-geostrophic balance is maintained over Central America as the Caribbean trade winds blow across the isthmus and over the eastern Pacific Ocean. The 2.5° × 2.5° resolution of the NCEP SLP fields analyzed in section 4 is too coarse to quantitatively test the validity of the geostrophic balance in the Papagayo gap. However, the speculation about the geostrophic nature of the Papagayo jet is consistent with the zonal alignment of the cross-isthmus contours of the correlation between Papagayo winds and SLP in the middle panel of Fig. 8 and the high correlation of 0.82 between Papagayo winds and the meridional pressure gradient in the Caribbean noted in section 4.

An inspection of the topographic map in Fig. 1 of CFE questions the validity of the above speculation. The width of the Nicaraguan lake district is comparable to that of the Panama gap, yet the tendency for anticyclonic turning of the Panama jet suggests that the inertial balance has relevance to the winds over the Gulf of Panama. The answer to this paradox may lie in the fact that the Panama gap is oriented from southwest to northeast but the winds are predominantly northerly in the upper reaches of the Gulf of Panama. The effective gap width perpendicular to northerly winds blowing across the Isthmus of Panama is therefore much narrower than the actual gap width.

Although there is no anticyclonic turning of the core of the Papagayo wind jet, the fanning of the wind field away from the jet axis is qualitatively similar to the fanning observed in the Tehuantepec and Panama wind jets. This is evident from the case study examples presented by CFE. An enlargement of the Papagayo region during the period 4–5 March 1997 in the March case study summarized in section 3c of CFE is shown in Fig. 16. The divergence of the fanning away from the axis of the jet near the coast is considerably weaker and more spatially variable than in the Tehuantepec and Panama examples presented in the previous sections. These characteristics of the divergence field are typical of the Papagayo wind jet over the NSCAT data record. The nearly zonal line of zero relative vorticity emanating from the Papagayo gap indicates that there was very little turning of the axis of the jet after leaving the coast in this particular event.

From the ECMWF maps of this March 1997 Papagayo wind event (right panels of Fig. 16), the fanning of the wind jet was well reproduced in the ECMWF analyses. However, the winds were much

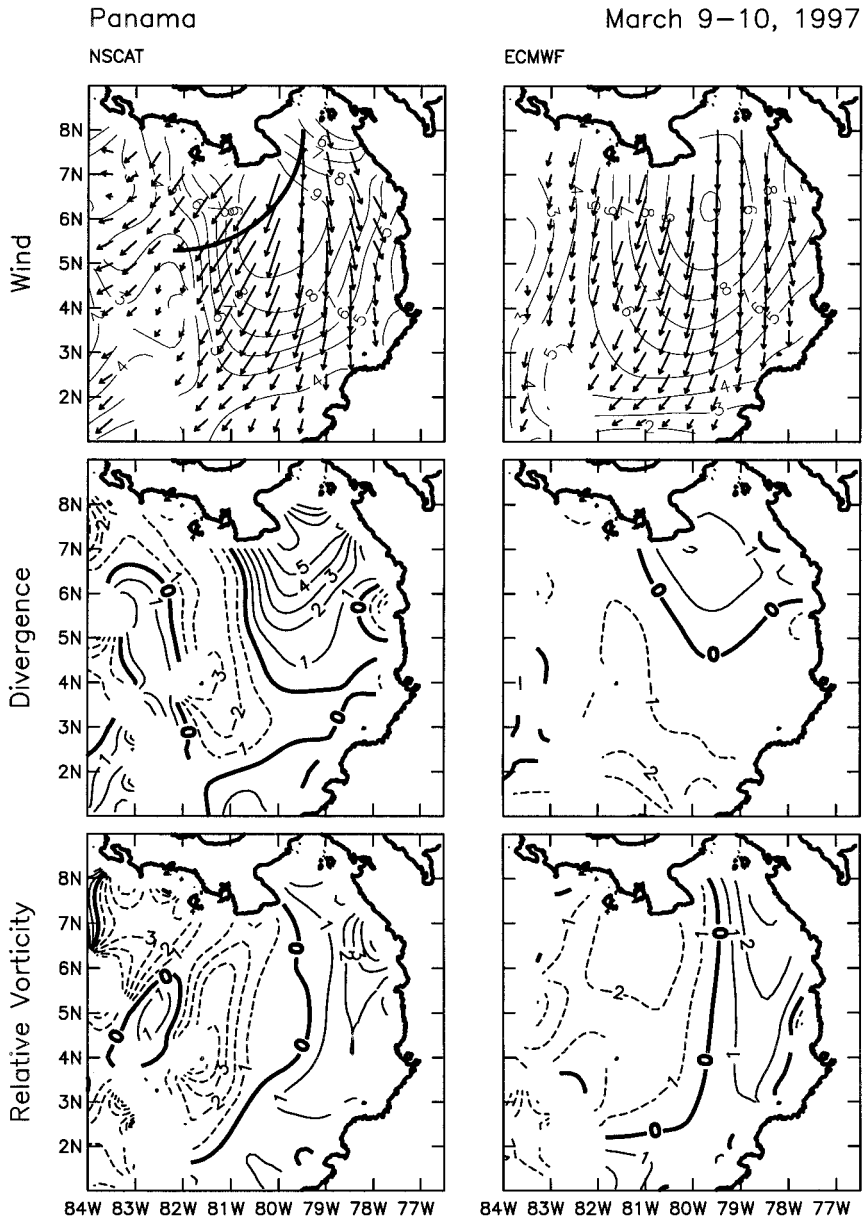

FIG. 15. Composite averages of (upper) the 10-m vector wind field, (middle) wind divergence, and (bottom) relative vorticity over the Gulf of Panama for the 2-day period 9–10 Mar 1997. (left and right panels) Constructed as in Fig. 11 and the heavy line in the upper-left panel is the inertial path originating at the gap opening with the observed wind speed at 15.25°N, 95°W, and a northerly direction.

more concentrated near the axis of the jet in the NSCAT observations, as evidenced by the band of stronger negative relative vorticity on the north side of the jet axis.

6. Discussion and conclusions

Satellite estimates of 10-m winds by the NASA scatterometer (NSCAT) were analyzed to investigate regional relationships between the three wind jets along the Pacific coast of Central America and the surface wind and pressure fields in the Inter-American Seas and eastern tropical Pacific. From the detailed overview of scatterometry and comparisons with buoy observations of 10-m winds in the appendix of the companion paper to this study (Chelton et al. 1999), we feel confident that the conclusions from the statistical analyses presented in this study are not artifacts of NSCAT measurement or sampling errors. Moreover, the ensemble of events observed during the 9-month NSCAT mission

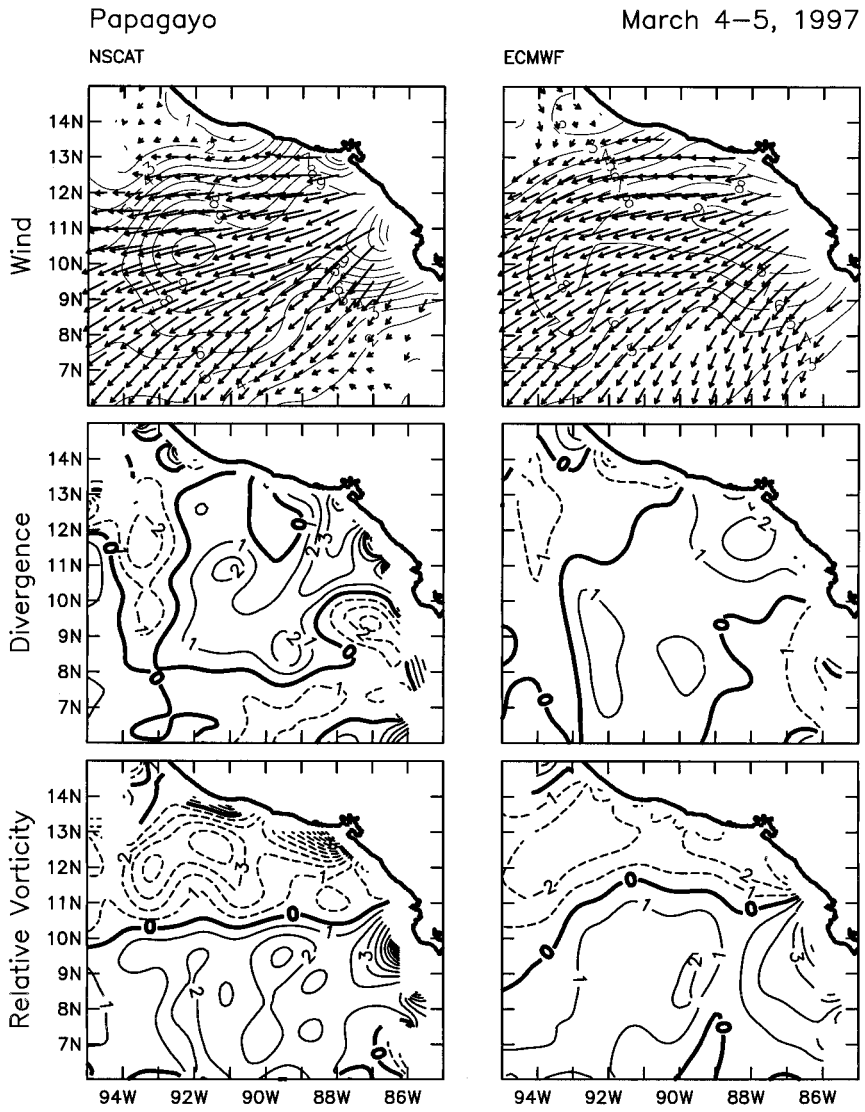

FIG. 16. Composite averages of (upper) the 10-m vector wind field, (middle) wind divergence, and (bottom) relative vorticity in the region of the Papagayo jet for the 2-day period 4–5 Mar 1997. (left and right panels) Constructed as in Fig. 11.

presumably sampled a wide range of stages of the development of the jets. We therefore believe that the statistics of the wind jets were adequately sampled by NSCAT.

Perhaps the most important conclusion of this study is that the NSCAT observations question the generality of the widely accepted view that the winds in the Papagayo and Panama jets are generated by high pressure systems of midlatitude origin that occur during winter and spring and sweep from northwest to southeast across the Inter-American Seas. Consistent with the conventional view, the Tehuantepec wind jet was driven by atmospheric pressure variations in the Gulf of Mexico. This was demonstrated from three case studies presented in CFE and from the statistical analysis of the relationship between the intensity of the jet and cross-isthmus pressure variations presented here in section 4. While the Papagayo and Panama jets were sometimes coupled to the Tehuantepec jet in accord with the conventional view (see the December 1996 case study and the early stages of the November 1996 case study described by CFE), variations in the intensities of these two low-latitude jets were not significantly correlated with Tehuantepec jet variations at any lag over the period of the NSCAT data record. At least during the October 1996–June 1997 NSCAT observational period, high pressure systems of midlatitude origin evidently seldom penetrated as far south as the Papagayo and Panama gaps.

The statistical analyses presented here suggest a different dynamical mechanism for generation of Papagayo and Panama jets. Variations in the intensities of these

two lower-latitude jets were correlated with variations in the trade winds of large zonal extent spanning from the Caribbean Sea across Central America into the eastern tropical Pacific.

The relationships between the three major wind jets and the surrounding wind field over the Inter-American Seas and eastern tropical Pacific are compactly summarized by the empirical orthogonal functions (EOFs) of the vector winds. The three most energetic EOFs and corresponding amplitude time series of the vector winds, after removal of the vector average wind at each location, are shown in Figs. 17 and 18. Cumulatively, these three modes account for about 42% of the variance summed over the $1° \times 1°$ grid.

The first EOF in the top panel of Fig. 17, which accounts for about 19% of the variance, is dominated by the Papagayo jet and its downstream extension to the northeast trade winds of the Pacific. Although the vector average wind at each $1° \times 1°$ grid location has been removed, the orientations of the vectors in this EOF are very similar to the orientations of the vector averages (see the top panel of Fig. 11 of CFE). This first EOF can therefore be interpreted as modulations of the intensity of the vector average wind field. The pattern of this EOF clearly illustrates the link between the Papagayo jet outflow and the Pacific trade winds. The amplitude time series of this first EOF (top panel of Fig. 18) shows a strong seasonal variation with a maximum in early March when seasonal variations of the Papagayo winds were strongest (see Fig. 13 of CFE). In association with the strong Papagayo outflow represented by this mode of variability, there are secondary maxima over the Gulfs of Panama and Tehuantepec. This first EOF thus captures primarily the correlated seasonal variations of the three jets (see Fig. 13 of CFE). Since the vector average velocity has been removed at each grid location for the EOFs presented here, the negative minima at the beginning and end of the 9-month data record are indicative of weakening of the vector average wind pattern during the fall and early summer. Superimposed on the strong seasonal variability, there were events with amplitudes comparable to the seasonal signal and timescales ranging from a few days to a week. The dominance and large zonal extent of the Papagayo jet in this first EOF are representative of the March 1997 case study considered by CFE.

The second EOF, accounting for 12% of the variance, is dominated by a broad band of southwesterly flow

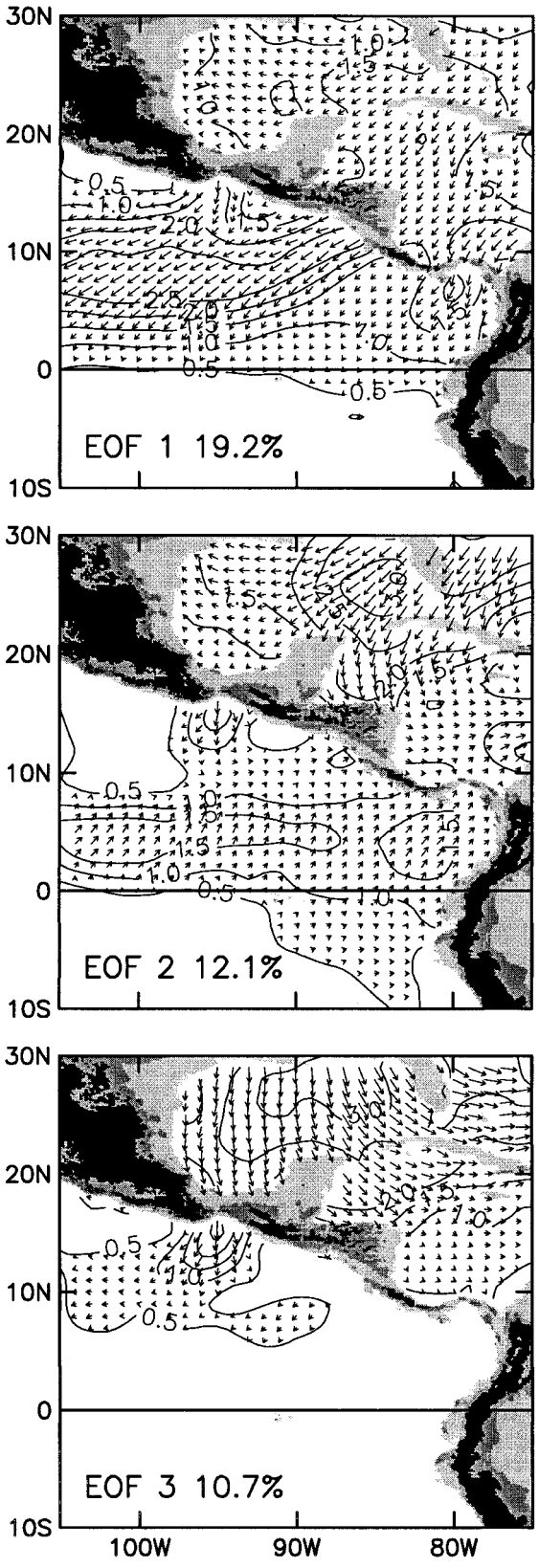

→

FIG. 17. The three most energetic vector empirical orthogonal functions (EOFs) from the covariance matrix of the two vector wind components in 2-day composite average fields on a 1° grid. The percentages of variance are labeled for each mode. The contours correspond to the magnitude of the vector EOF at each grid location. For clarity of presentation, vectors are shown only at those grid locations for which the magnitude of the vector EOF exceeds 0.5. The topographic gray shades are as in Fig. 1.

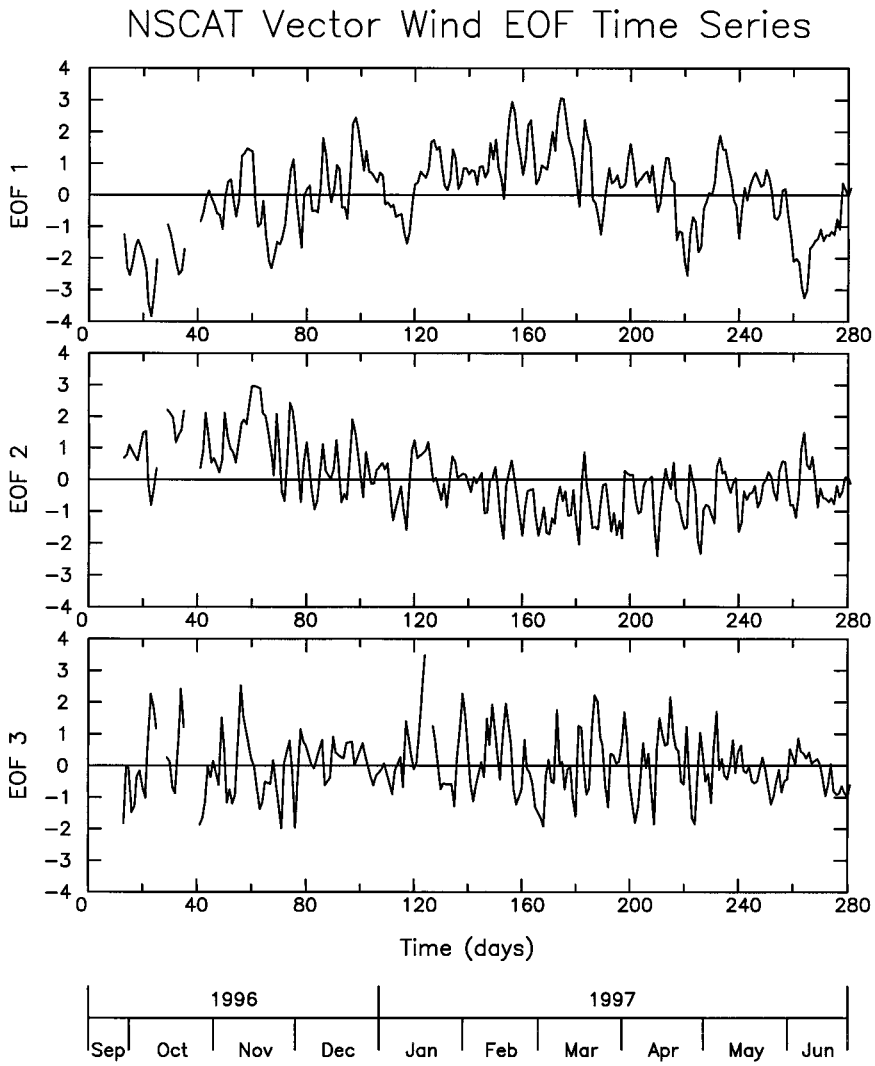

FIG. 18. The amplitude time series of the three most energetic vector EOFs shown in Fig. 17. Owing to the irregular data gaps in the wind time series at each 1° grid location over the domain of interest, it was necessary to objectively estimate the value of the amplitude time series as described in Davis (1976) at times when any of the grid points were missing data. Because the spatial scales of these three dominant EOFs are so large, the amplitude time series could be accurately estimated from the subset of grid points with nonmissing data values on each given day.

with the strongest winds in a band between about 3°N and 6°N across the entire domain of interest. Among the three modes shown in Fig. 17, this is the only mode with significant cross-equatorial flow. In association with this cross-equatorial flow, the Papagayo and Panama winds are onshore. The Tehuantepec jet blows offshore in this mode of variability, but the flow becomes westerly south of about 13°N. The amplitude of this mode was largest during the first 2 months of the data record when the Central American monsoon was still active. The pattern of the wind field in this second mode resembles the late stages of the November 1996 case study summarized by CFE.

The third EOF, accounting for 11% of the variance, is representative of the classic Tehuantepec wind event. The Tehuantepec jet turns anticyclonically toward the west and fans away from the axis of the jet. These wind variations over the Gulf of Tehuantepec are coupled with strong northerly winds over the western and central Gulf of Mexico and broad cyclonically turning winds over the northeast quadrant of the domain of interest. However, there is no associated variability over the Gulfs of Papagayo or Panama, indicating that this pattern of the Tehuantepec wind jet blows independently of the Papagayo and Panama wind jets. This third EOF was very energetic during the first 2 months of the data record and became weak during December. The variability was energetic again from mid January until early May.

The structures of the winds within the cores of the three jets were examined in section 5 to investigate dynamical balances within each individual jet. A detailed analysis of the structure of the Tehuantepec wind jet in section 5b concluded that the jet axis was consistent with an inertial path near the coast for sufficiently high wind speeds. With increasing distance from the coast, however, the anticyclonic turning of the Tehuantepec jet was almost always less than that of an inertial jet. It was therefore concluded that geostrophic adjustment plays an important role in the dynamics of the Tehuantepec jet after it leaves the coast, ultimately causing the jet to become easterly in approximate geostrophic balance at about 10°N.

The Panama wind jet is similar in some respects to the Tehuantepec jet, although the Panama jet is much less intense and the anticyclonic turning is often disrupted by the large-scale southwesterly cross-equatorial flow that is common in the far-eastern tropical Pacific.

The Papagayo jet shows no tendency toward anticyclonic turning, clearly indicating that this jet is dynamically different from the Tehuantepec and Panama jets. It was suggested that the different character of the Papagayo jet may be because the gap over the Nicaraguan lake district is wide enough for the trade winds to maintain a near-geostrophic balance across Central America.

A robust feature of the observations that merits special attention is the fanning on the east sides of the Tehuantepec and Panama wind jets. The NSCAT measurements consistently show much stronger fanning than is present in the ECMWF analyzed wind fields. The bias toward northerly winds with little or no westerly component in the ECMWF analyses is very similar to that found in a recent mesoscale model simulation of a March 1993 Tehuantepec wind event (Steenburgh et al. 1998). The momentum budget in the Steenburgh et al. analysis can therefore shed light on the discrepancies between the NSCAT observations and the ECMWF analyses. There is evidently excessive westward acceleration in the ECMWF and mesoscale models, possibly resulting from systematic errors in the model parameterizations of boundary-layer processes.

It is hoped that the NSCAT observations described here will motivate an investigation of model dynamics and lead to improved parameterizations so that the models more faithfully reproduce the observations. Mesoscale modeling studies would yield further insight into the trade wind mechanism proposed here for the generation of the Papagayo and Panama jets. Such modeling could also determine the dynamical balances that are responsible for the lack of anticyclonic turning of the Papagayo jet.

In closing, we note that the much broader measurement swath of the next-generation QuikSCAT scatterometer that was recently launched in June 1999 will greatly reduce the sampling limitations of NSCAT data. The average revisit interval at 15° lat will be reduced from 23.5 hours for NSCAT to 19 h for QuikSCAT. Overlap of the QuikSCAT mission with the identical broad-swath Sea Winds scatterometer scheduled for launch in November 2001 offers the prospect of reducing this revisit interval to 9 h. Such frequent sampling approaches the 6-hour synoptic period for global weather analysis and forecast models, thus promising to revolutionize studies of the space–time variability of the surface wind field.

Acknowledgments. We thank Michael Schlax for preparing the figures and for many helpful discussions and suggestions that greatly improved the manuscript, Dean Vickers for help with the NCEP sea level pressure analyzed in section 4, and Horst Boettger, Tony Hollingsworth, and John Henessey for their generosity and help in making the 1° × 1° × 6-h gridded operational ECMWF analyses of 10-m winds available for the analyses in section 5. We also thank David Schultz and an anonymous reviewer for their careful reading of the manuscript and constructive suggestions for improvement. The research presented in this paper was supported by Contracts 957580 and 959351 from the Jet Propulsion Laboratory funded under the NSCAT Announcement of Opportunity and NOAA Grants NA56GP0208 and NA76GP0404 from the Office of Global Programs.

REFERENCES

Barton, E. D., and Coauthors, 1993: Supersquirt: Dynamics of the Gulf of Tehuantepec, Mexico. *Oceanography*, **6,** 23–30.

Breaker, L. C., W. H. Gemmill, and D. S. Crosby, 1994: The application of a technique for vector correlation to problems in meteorology and oceanography. *J. Appl. Meteor.*, **33,** 1354–1365.

Chapel, L. T., 1927: Winds and storms on the Isthmus of Panama. *Mon. Wea. Rev.*, **55,** 519–530.

Chelton, D. B., 1983: Effects of sampling errors in statistical estimation. *Deep-Sea Res.*, **30,** 1083–1103.

——, M. H. Freilich, and S. K. Esbensen, 2000: Satellite observations of the wind jets off the Pacific coast of Central America. Part I: Case studies and statistical characteristics. *Mon. Wea. Rev.*, **128,** 1993–2018.

Clarke, A. J., 1988: Inertial wind path and sea surface temperature patterns near the Gulf of Tehuantepec and Gulf of Papagayo. *J. Geophys. Res.*, **93,** 15 491–15 501.

Crosby, D. S., L. C. Breaker, and W. H. Gemmill, 1993: A proposed definition for vector correlation in geophysics: Theory and application. *J. Atmos. Oceanic Technol.*, **10,** 355–367.

Davis, R. E., 1976: Predictability of sea surface temperature and sea level pressure anomalies over the North Pacific Ocean. *J. Phys. Oceanogr.*, **6,** 249–266.

Frankenfield, H. C., 1917: ''Northers'' of the Canal Zone. *Mon. Wea. Rev.*, **45,** 546–550.

Freilich, M. H., and R. S. Dunbar, 1999: The accuracy of the NSCAT-1 vector winds: Comparisons with National Data Buoy Center buoys. *J. Geophys. Res.*, **104,** 11 231–11 246.

Holton, J. R., 1992: *An Introduction to Dynamic Meteorology.* Academic Press, 507 pp.

Hurd, W. E., 1929: Northers of the Gulf of Tehuantepec. *Mon. Wea. Rev.*, **57,** 192–194.

Jupp, P. E., and K. V. Mardia, 1980: A general correlation coefficient for directional data and related regression problems. *Biometrika*, **67,** 163–173.

Kalnay, E., and Coauthors, 1996: The NCEP/NCAR 40-Year Reanalysis Project. *Bull. Amer. Meteor. Soc.,* **77,** 437–471.

Overland, J. E., 1984: Scale analysis of marine winds in straits and along mountainous coasts. *Mon. Wea. Rev.,* **112,** 2530–2534.

——, and B. A. Walter Jr., 1981: Gap winds in the Strait of Juan de Fuca. *Mon. Wea. Rev.,* **109,** 2221–2233.

Parmenter, F. C., 1970: A ''tehuantepecer.'' *Mon Wea. Rev.,* **98,** 479.

Roden, G. I., 1961: On the wind-driven circulation in the Gulf of Tehuantepec and its effect upon surface temperatures. *Geofis. Int.,* **1,** 55–76.

Schultz, D. M., W. E. Bracken, L. F. Bosart, G. J. Hakim, M. A. Bedrick, M. J. Dickinson, and K. R. Tyle, 1997: The 1993 superstorm cold surge: Frontal structure, gap flow and tropical impact. *Mon Wea. Rev.,* **125,** 5–39; Corrigenda, **125,** 662.

——, ——, and ——, 1998: Planetary- and synoptic-scale signatures associated with Central American cold surges. *Mon. Wea. Rev.,* **126,** 5–27.

Steenburgh, W. J., D. M. Schultz, and B. A. Colle, 1998: The structure and evolution of gap outflow over the Gulf of Tehuantepec, Mexico. *Mon. Wea. Rev.,* **126,** 2673–2691.

Trasviña, A., E. D. Barton, J. Brown, H. S. Velez, P. M. Kosro, and R. L. Smith, 1995: Offshore wind forcing in the Gulf of Tehuantepec, Mexico: The asymmetric circulation. *J. Geophys. Res.,* **100,** 20 649–20 663.